POLITECNICO DI TORINO

Master's Degree in Physics of Complex Systems

Master's Degree Thesis

The nucleus as a regulator of the cell cycle

How mechanical perturbations affect the length of the G1 phase

Supervisors

Prof. Jean-François JOANNY

Prof. Davide AMBROSI

Candidate

Caterina COCCA

July 2023

Abstract

Regarded as the seed of any form of life, the cell is a complex and stunning system capable of performing a great variety of tasks. In order to properly complete its functionalities, precise mechanisms of control are necessary during the cell life (i.e. the cell cycle). Among them, great importance is given to the ones related to size homeostasis; indeed, experimental evidence has shown that size is cell type specific and is important in monitoring cell function.
The actual state of knowledge in the field has identified three main 'checkpoints' for this regulation: the reduction or starting point, at the G1/S transition, which defines the border between growth and DNA replication; a checkpoint at the G2/M transition, which is related to the division between the pre-mitotic phase and the mitotic one; and the spindle checkpoint that ensures the correct progress of the mitotic phase.
The former has attracted great interest already in the past since the length of the G1 phase seems to be the most variable during the cell cycle.
Experimental observations have demonstrated that the compression of the nucleus is fundamental to undergo the G1/S transition and that this flattening is strictly connected to a delicate balance of fluxes of metabolites inward and outward of the nucleoplasm.
This work will present the theoretical grounds of the hypothesis suggested by the team of Matthieu Piel at the Institute Curie (Paris): the nuclear tension is proposed as a key parameter that couples cell size homeostasis and cell cycle length regulation. The analyses of this tension and how it affects the nuclear shape, the hypothesis of a critical value for the tension that triggers the G1/S transition and its connection with the variability of duration of the G1 phase are the main subjects of this study which allow to go deeper into the understanding of the cell cycle and of the diseases related to its misfunction.

Acknowledgements

Complicare è facile, semplificare è difficile.

Per complicare basta aggiungere (...). Tutti sono capaci di complicare. Pochi sono capaci di semplificare.
(...)
Per semplificare bisogna togliere, e per togliere bisogna sapere cosa togliere, come fa lo scultore quando a colpi di scalpello toglie dal masso di pietra tutto quel materiale che c'è in più della scultura che vuole fare. Teoricamente ogni masso di pietra può avere al suo interno una scultura bellissima, come si fa a sapere dove ci si deve fermare per togliere, senza rovinare la scultura?
(...)
Togliere invece che aggiungere vuol dire riconoscere l'essenza delle cose e comunicarle nella loro essenzialità. Questo processo porta fuori dal tempo e dalle mode.
Il teorema di Pitagora ha una data di nascita, ma per la sua essenzialità è fuori dal tempo. Potrebbe essere complicato aggiungendogli fronzoli non essenziali secondo la moda del momento, ma questo non ha alcun senso secondo i principi della comunicazione visiva relativa al fenomeno.
(...)
La semplificazione è il segno dell'intelligenza, un antico detto cinese dice:
"Quello che non si può dire in poche parole non si può dirlo neanche in molte".

Bruno Munari, *'Verbale Scritto'*, 1982

A Puff, alla mia famiglia
e a tutti coloro che ho incontrato nel mio percorso.

Table of Contents

List of Tables

List of Figures

Chapter 1

Introduction

1.1 Cells growth and cell size regulation

In recent years great interest has been directed towards the application of physical tools to the study of cell growth, division and proliferation. A well-established mechanism to control cell growth is related to cell size regulation, whose importance goes beyond cell proliferation, being present also in non-proliferating cells (e.g. neurons)[1]. Indeed, despite the great variety of size across cell types, with volumes ranging over 14 orders of magnitude (from 0.1 femtoliter ultramicro bacteria to 10 milliliter amoebae cells) [2] [3], cells of the same type usually exhibit uniformity of size [4] [5] [6] with populations of cells regularly exhibiting 10% variance in size at division [2].

However, the study of cell size regulation is a great challenge. The specific size of a cell is the result of a variety of complex and coupled processes: cell volume variations during growth and motility [7]; cell mass density homeostasis, which is related to a cell's metabolic and anabolic activity [8]; protein turnover and the scaling between proteins and small osmolytes, mainly amino-acids and ions [9] [10]; balance between growth and division [11].
As a consequence, there is still lack of a clear and complete understanding of the mechanisms that control cell size and their relation with the cell cycle progression.

In mammalian cells, size regulation has been proven to play a key role in cell cycle regulation by triggering the G1/S transition, a stage at the boundary between the phase in which the cell grows and the one devoted to DNA replication (see figure 1.1 and Appendix D for more details).
Inside the eukaryotic kingdom, studies on yeast have shown the existence of cell-autonomous size control mechanisms.
The first evidence of cell size checkpoints in the cell cycle of both budding yeast and

fission yeast was observed in 1977 [12] [13]. Experiments on both species proved that the length of the cell cycle is influenced by cell size: it is extended in small cells, giving them more time to grow before their next division, while larger cells grow less to prevent themselves from becoming excessively large [5].

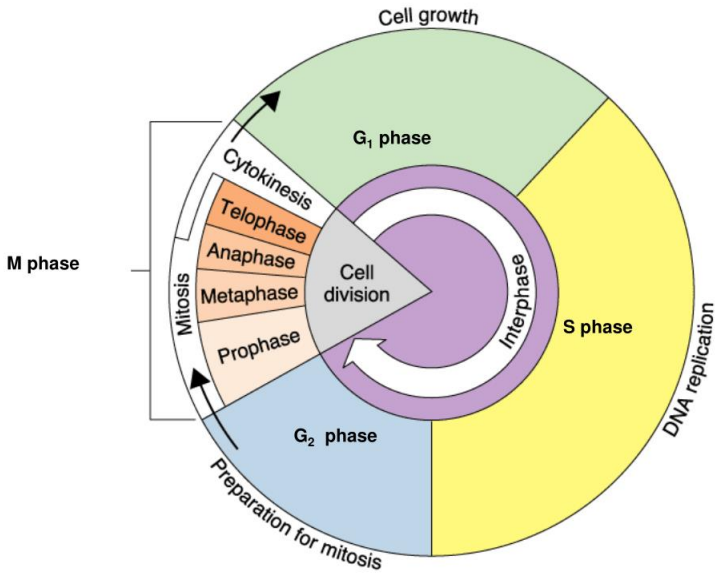

Figure 1.1: The cell cycle and its phases. Adapted from iBiology[14].

Similar evidence in mammalian cells [4] have led to the development of different models to explain the coupling between cell cycle and cell size; three main coarse-grained models, which analyze the cell volume at various stages of the cell cycle considering the cell as a whole, have been proposed [15] [4] (see figure 1.2):

1. sizer (first proposed in the 1970s [12] in fission yeast and budding yeast daughter cells, recently proposed also for cell differentiation in plants [16]), where cells divide after reaching a certain target size whose value is fixed and is equal for all the cells independently from their birth size.
   Typical of this model is the negative correlation between size at birth and added size during growth but the absence of correlation between initial and final volume;

2. adder(e.g. in bacteria, cyanobacteria and in budding yeast [17]), in which cells divide after a specific amount of cell size (either cell volume or cell surface area) is added, independently of their birth size. The result in this case is the absence of a correlation between size at birth and added volume but a positive correlation between initial and final volume;

3. timer(e.g. in Caulobacter crescentus [18]), whose transition criterion is the time spent in the different cell cycle phases. The correlation between size at birth and size added during growth is positive for cells growing exponentially as well as the correlation between the initial and the final volume.

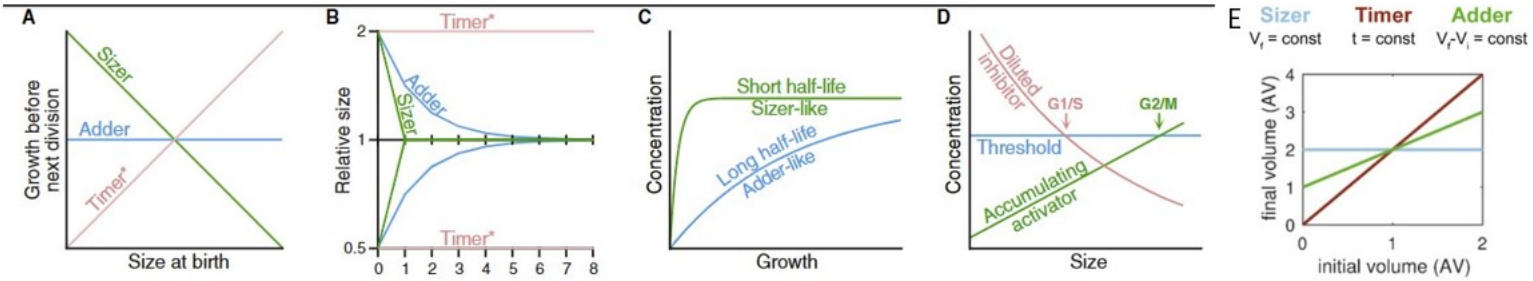

Figure 1.2: Models for size regulation. (A), (B), (C) and (D) adapted from Rhind[2]. (E) adapted from Heldt[19].

((a)) Correlation between size at birth and growth in the subsequent cell cycle.

((b)) Kinetics of return to size homeostasis. Adders return to their target size more slowly than sizer, which usually requires just one generation to come back to their target size since cells only double their volume before division; timer do not enforce size homeostasis, cells divide at the same size their parents divided.

((c)) Half-life of division-proteins in the case of sizer and adder. The half-life of a protein represents the time it takes to reach a steady state thanks to the balance between synthesis and degradation. This picture shows the different way in which a protein reaches its steady state with either a sizer mechanism or an adder one: in the first case, a protein has a shorter half-life and quickly reaches the steady state with no dependence on the amount of growth; in the latter, instead, a longer half-live implies proportion with the amount of growth and not to the size.

((d)) Kinetics of size-protein : inhibitor-dilution and activator accumulation. Here the first model is depicted for the G1/S transition, as proposed for budding yeast, while the second one is for the G2/M transition, as proposed for fission yeast. Even if shown in the same graph, these two mechanisms usually do not happen in the same cell and simultaneously.

((e)) Theoretical predictions of final volume (V_f) over the initial volume (V_i) for an ideal sizer, timer and adder in arbitrary units of volume (AV).

Nowadays the model that seems more realistic tries to reconcile sizer concepts at the single cell level with an adder-like behaviour at a population level [20].
A timer mechanism that assumes exponential growth seems theoretically incompatible with the experimental observation of a small variance in cell size distributions

because it would lead instead to the divergence of this variance [21].

Considerable questions complicate this problem. The first issue comes from the definition of the concept of size itself; indeed, cell size is determined by different parameters(e.g. volume, length, surface area, protein content, mass, density and growth rate) whose correlation is relevant but complicated. Secondly, it is important to distinguish between how cells determine their target size and how they maintain homeostasis at that target size.

In this work, the idea that volume is the key phenomenological variable controlling cell size [22] will be explored and the focus will be on the mechanism that allows cells to maintain their homeostasis.

Several hypotheses have been suggested to explain the size regulation mechanism: on the one side, a great variety of biochemical pathways have been proven to be key determinants of cell size (e.g.cyclins and cyclin-dependent kinases (CDKs) [23] and IGF/PI3K/AKT/mTORC1 pathway [15] [24] [25]); another type of biochemical origin is the presence of sizer proteins whose variations in concentration, either a decrease (inhibitor-dilution model, e.g.Rb e Wh5) or an increase (activator accumulation), may trigger the transition between different steps of the cell cycle [26] [27] [2]; on the other hand, the well-established importance of mechanical stress in cell homeostasis [28] seems to suggest a possible mechanism of cell cycle regulation (and specifically G1 length regulation) related to mechanical forces (see figure 1.3).

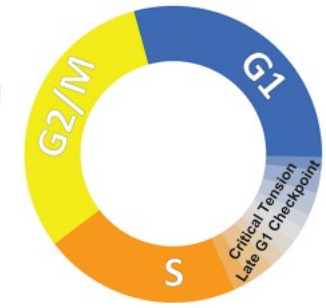

Figure 1.3: Phases of the cell cycle. The connection between mechanical stress and G1/S transition checkpoint is highlighted. Adapted from Perez[28].

1.2 Aim of the thesis

The goal of this work is to explore a new hypothesis to explain cell size homeostasis and cell cycle duration, with particular attention to the role played by the cell nucleus. The nucleus, the largest organelle in the cell, represents a good mediator for the transmission and modulation of mechano-sensitive processes; indeed, nucleus deformation has been shown to have influence on a great variety of processes: nuclear transport [29], cell differentiation, chromatin organization [30], migration and pathfinding in constrained environments [31] [32].

Following the idea of a relation between cell cycle regulation and nucleus deformation, **Chapter 2** is divided into two different sections devoted to the explanation of experimental and theoretical evidence that supports the idea of a relation between mechanical perturbations and cell cycle regulation.
On the theoretical side, the starting point is a model presented in Rollin[10] to derive the physical basis of cell size regulation. Two subsections describe the theoretical grounds of this model:

- the Pump-Leak model, which succeeds in defining the scaling laws for the volume of the cell in relation to the scaling between proteins and small osmolytes, mainly amino-acids and ions;

- a model of stochastic gene expression and translation, whose aim is to couple mRNA and protein production rate to cell growth and homeostasis.

As a consequence of this model, particular attention is given to the nuclear-to-cytoplasmic ratio (NC), also known as karyoplasmatic ratio. The fact that it remains almost constant during growth [33] [34] may be a hint of a role played by the nucleus in maintaining cell homeostasis.

The second part of this work is therefore focused on the analysis of the behaviour of the cell nucleus under the effects of different mechanical stresses, emulating what happens during the G1/S transition. The attention is directed towards the understanding of how the nucleus deformations could be the key factors to trigger cell division and regulate the time spent in the G1 phase. More in details, in **Chapter 3** we derive an analytic formula for the metabolites inside the nucleus in several regimes and for the hydrostatic pressure at the NE related to them in order to couple it to the nuclear tension. **Chapter 4** introduces a non-linear elastic model of the nuclear envelope (NE) in order to theoretically understand the origin of the tension which experimentally seems to strongly affect the cell cycle and its length regulation. **Chapter 5** of this thesis follows this hypothesis by proving the dependence of the time spent in the G1 phase on the nucleus size and, as a

consequence, on the tension at its membrane. Space for a final discussion of the results is left in the **Conclusion**.

Chapter 2

Experimental and theoretical basis

2.1 Experimental evidence

The hypothesis suggested in this work is based on the idea that the G1 length, therefore the cell size homeostasis, has a connection with mechanical perturbations and this mechanical stress is sensed by the cell via the nucleus.

In the last years, several experiments have demonstrated the key role played by the nucleus in the response to spatial confinement.
In particular, this work is motivated by the following results:

- Lomakin et al.[31] have proven the ability of a single cell to sense confinement through its nucleus and respond by activating several biochemical pathways;
- Aureille et al.[35] have shown the G1/S transition to be triggered by the flattening of the nucleus;
- Skotheim et al. [26] have demonstrated that the cell cycle progression is strictly related to changes in the concentration of proteins inside the cytoplasm.

More in details, Lomakin et al.[31] have studied a human cell line, HeLa cell, under the effect of controlled confinement thanks to the use of an ion beam-sculpted flat silicon microcantilever mounted on an atomic force microscopy (AFM). These measurements suggest that cells are able to detect their height and trigger contractile response below a threshold value of this height. The key element that makes the single cell capable of proprioception seems to be the nucleus. Indeed, enucleated cells (produced by centrifugation) showed defective contractile response

to spatial confinement.
Two different regimes of response can be identified (see figure 2.1):

1. above the threshold height, a "safe" regime, where the nucleus maintains a constant volume. The confinement in this case has the effect of unfolding the NE and increasing the surface area.

2. below the threshold height, identified for this cell line at a value of 5μm, during which nuclear folds are completely stretched, the nuclear envelope (NE) starts to be tensed and compression results in nuclear volume loss.

Overall, this study highlights the critical role of the NE in responding to mechanical signalling. Indeed, in the safe regime, i.e. $h = 20\mu m$, the force applied on the nucleus results as a constant $\sim 20nN$; whereas, after confinement at the critical value of $h = 5\mu m$, the force increased up to $\sim 80nN$, with a variation $\Delta F \sim 50nN$ on average.

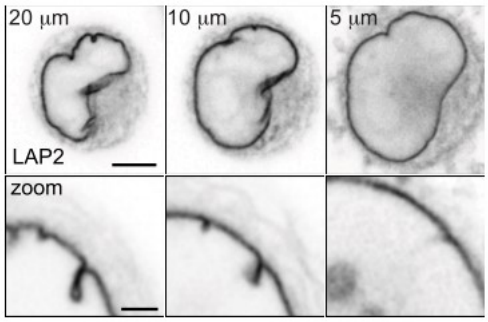

Figure 2.1: Effect of confinement on the nucleus. The pictures show the unfolding of the NE at different height (20μm, 10μm and 5μm, from left to right). Adapted from Lomakin[31].

Following the results from Aureille et al. [35], Matthieu Piel's team at the Institute Curie (Paris) has started to focus on the effect of confinement during cell growth. This thesis is aimed to theoretically analyze the unpublished results obtained in this study.

The most relevant outcome for this work stands in the discovery of a relation between cell size at birth and the duration of the G1 phase: cells born bigger spend less time in the growing phase G1, while smaller cells need more time to grow and to reach the threshold parameters that trigger the G1/S transition (see figure 2.2). Motivated by the aforementioned cell size sensing mechanism, the focus of this

thesis is oriented towards the role of the nuclear tension to explain this variance in the G1 duration. In particular, the presence of folds at the NE is identified as determinant to explain the response of the nucleus to mechanical stress and confinement. The idea proposed by Piel's team is that these folds act as a surface "reservoir" for the nucleus; as a consequence, in bigger cells, where the folds are already stretched, a shorter period of time is needed to enter the S phase, whereas in smaller cells, where the NE presents more folds, a longer G1 is necessary to reach the threshold value of the nuclear tension to trigger the G1/S transition.

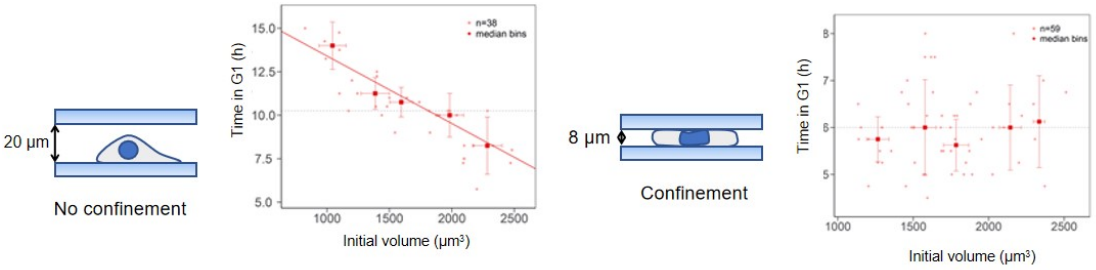

((a)) Cell growth during the G1 phase with and without confinement. Without confinement cells show a difference in the G1 length depending on their size at birth. Below a threshold confinement, this difference disappears and the minimum time in G1 is of ~ 6 hours independent from the volume at birth.

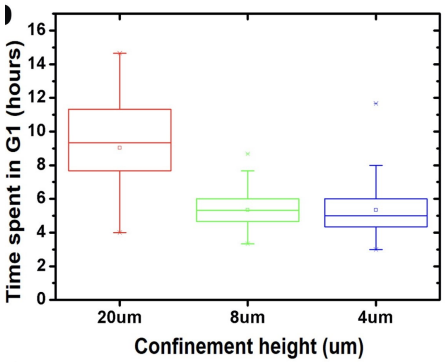

((b)) The effect of different confinement on the G1 length. A critical value of the height of confinement can be identified at around 8μm below which the G1 phase does not change its length.

Figure 2.2: Results from the experiment run at Matthieu Piel's lab in Paris (Institute Curie).

An additional question is then related to the origin of this nuclear tension and to the presence of a minimal time in G1 which does not depend on the cell volume and on the height of confinement if below a certain threshold. The answer suggested by

Piel's team follows the results presented by Skotheim et al. [26].

Skotheim et al.[26] have identified the presence of a specific protein in mammalian cell, Rb, which is not synthesized during cell growth. The fact that this protein does not scale with cell size implies it is diluted by cell growth. Therefore, Skotheim et al. suggested that Rb in mammalian cells can play the role of cell cycle inhibitor and trigger the G1/S transition when it reaches a specific concentration.

Therefore, the suggestion of Piel's team is that the presence of a minimal time spent in the G1 phase is due to the existence of an inhibitor protein that requires a minimal period of time to reach the amount of concentration that allows the cell to progress in its cycle. Whether this protein is Rb or a different one, it is still an open question. Ginzberg et al. [36] suggested Rb to be determinant in specifying the target cell size, but not in the coordination of growth rate with cell cycle length to reach cell size homeostasis.

Based on these observations, the next chapter will start by presenting the theoretical physical basis of cell size scaling during growth and its connection to protein production, which will be the first step towards the understanding of nuclear scaling and its relation with nuclear tension as the G1 length control parameter.

2.2 Physical basis of cell growth and homeostasis

The volume is an important parameter both for the physics and for the physiology of the cell. Its scaling during cell growth is strictly related to a cell type specific constant density as the result of the coordination of RNA and protein synthesis with cell volume increase.
Indeed, being negatively charged, RNA and proteins affect osmolarity indirectly and control water influx and cell volume increase through a mechano-osmotic process. This evidence can be explained through the so-called Pump-Leak model thanks to three main physical properties: electroneutrality, the balance of water chemical potential, and the balance of ionic fluxes.
The combination of this model with a model of stochastic gene expression is suited to describe the specific growth of cell volume during the cell cycle and the scaling of proteins and mRNAs (messenger RNA).
This section is devoted to the description of these models and their results.

2.2.1 Pump-Leak model

First proposed in 1960 [37], the Pump-Leak mechanism(PLM) is a mathematical model which describes how cells actively maintain an osmotic equilibrium with their environment. After water, Na^+, K^+, Cl^- are the most abundant ions in the extra and intracellular liquids [38] [39](see table 2.1) and the primary contributors to extra and intracellular tonicity; as a consequence, the regulation of their concentrations is a key factor for several cell activities (e.g. cell signalling [40] and cell volume stabilization [41]).

Ion concentration(mM)	*E.coli*	*S.cerevisiae*	mammalian cell(heart or RBC)
Na^+	10	30	10
Cl^-	10-200	5-100	100
K^+	30-300	300	100

Table 2.1: Ionic concentrations in a bacterial, yeast and inside a mammalian cell. RBC stands for red blood cells. Taken from Milo [38].

The presence of an imbalance in the concentration of sodium and potassium ions inside and outside the cell has been discovered by Carl Schmidt (1850) [42], but it was only in 1957 that Skou[1] introduced the idea of the Na^+ pump (Na^+/K^+ ATPase [NKA]) and of a relation between ion content and volume regulation in the cell [43].

[1]Nobel Prize in Chemistry in 1997 because of his discovery of the NKA.

Leaving aside the interesting history behind this discovery, the role of these ions can be understood by studying a simplified system: a spherical cell (e.g., a mitotic cell or a cell in suspension) with inside Na^+, K^+, Cl^-, water and impermeant macromolecules, X, such as proteins and metabolites, with an average charge valence z. In the text, capital letters (e.g. X) stand for the number of metabolites while the corresponding lowercase letters represent concentrations (e.g. $x = \frac{X}{V}$).

Following this description, it is possible to identify the components of the PLM (see figure 2.3(a)):

- a semipermeable and flexible membrane that can be crossed by Na^+, K^+, and Cl^-;
- impermeant molecules with negative net charge trapped inside the membrane;
- an energy consuming pump which drives Na^+ out of the membrane against the ionic gradient.

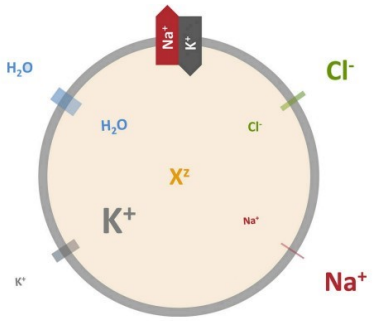

((a)) Main components of the Pump-Leak model. Na^+, K^+, and Cl^- are asymmetrically distributed in the outer and inner space of the cell. A semi-permeable membrane allows the flow of these ions while trapping inside in the cytoplasm impermeant molecules X with average charged z. Adapted from Kay [39].

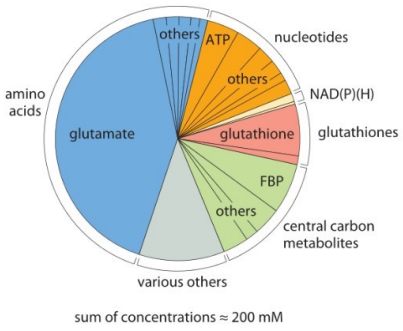

((b)) Composition of free metabolites in an *E.coli* cell growing on glucose. Adapted from Bennett [44].

Figure 2.3: PLM mechanism and the composition of amino-acids inside the cell

Mathematically, in the frame of a quasi-static theory (by assuming that the water flux balances instantaneously, which is valid on the timescale of minutes), the PLM can be expressed as a set of three coupled differential equations (see appendix

B for more details about the derivation) :

$$n^+ - n^- - z \cdot x = 0 \tag{2.1}$$

$$\Delta P = \Delta\pi = kT \cdot (n^+ + n^- - 2n_0 + x) \tag{2.2}$$

$$n^+ \cdot n^- = \alpha_0 \cdot n_0^2 \quad with \quad \alpha_0 = e^{-\frac{pkT}{g^+}} \tag{2.3}$$

where n^+, n^- and $2n_0$ are the concentrations of cations and anions inside and outside the cell and ΔP and $\Delta\pi$ represent the hydrostatic and the osmotic pressure difference respectively (i.e. $\Delta P = P_{in} - P_{out}$). α_0 is called pumping efficiency; this value is dimensionless, usually in a range between 0 (no pumping) and 1 (perfect pumping) and it is related to the pumping flux of cations p and their conductivity g^+. The typical values of these parameters are listed in table 2.2.
A table with the symbols used in this work can be found in Appendix A.
In the rest of the report, the composition of the solution in the extracellular space is considered fixed, which is reasonable since the the volume of the extracellular space is far larger than that of a single cell. Moreover, spatial effects will be neglected and it will be assumed that the cell can be considered a single isopotential sphere (i.e. all points within the cell are at the same potential) and the voltage in the extracellular space is null.

Parameter		Value
n_0	Concentration of metabolites outside of the cell [38]	150 mMol
n^+	Cations concentration[38]	160mMol
n^-	Anions concentration[38]	20 mMol
x	Metabolites concentration	120 mMol
z	Metabolites average charge	-1.2
ΔP	Difference in hydrostatic pressure	10-100 Pa
π	Osmotic pressure inside the cell	7.5x10^5 Pa
π_0	Osmotic pressure outside the cell	7.5x10^5 Pa
kT	Thermal energy at T=300K	4.1 pN.nm
K	Stretching modulus of the lamina	25 mN/m
α_0	Pumping efficiency	0.14

Table 2.2: Values of the coarse-grained parameters in the classical Pump-Leak model and in the nested Pump-Leak model.

These equations come from the following physico-chemical constraints on cells:

- Electroneutrality: equation 2.1 imposes electroneutrality inside the cell, i.e. a neutral mean charge; it is justified by the presence of a Debye length (used in plasmas and electrolytes to state the length scale at which the effect of

a charge persists) of the order of nanometers [45], much smaller than the micrometer scale of the cell volume.

- Osmotic balance: from van 't Hoff formula[2], equation 2.2 stands for the osmotic balance, i.e. the balance of water chemical potential between two sides of a semipermeable membrane. Despite the importance of water flux, there is still lack of clear understanding of the molecular basis of osmosis [39].

- Balance of ionic fluxes: the third equation 2.3 is related to the balance of ionic fluxes and comes as a result of the mass-action law (see appendix A1 for more details).

Therefore, the role of NA/K pump and of the membrane voltage in maintaining cell volume homeostasis can be understood as the consequence of two forces: concentration and electrical gradient.
Impermeant molecules X create an imbalance of charge known as Donnan effect[46]. From equation 2.1 we can see that these molecules attract counterions to preserve electroneutrality, i.e. they attracts cations inside the cell. As a consequence of this flux, the right term in equation 2.2 increases and a change in the left term is necessary to reach osmotic balance. Thus, if unregulated, this effect will lead to cell volume increase due to the osmotic flux of water inside the cell and its consequential lysis.
Indead, the pressures created by the osmolarity differences between inside and out can easily reach an atmosphere or more.
Plants and bacteria cells avoid this effect of the osmotic influx of water by building cellulose walls that can sustain high values of pressure [47]. Animals, instead, whose plasma membrane is only about as strong as a soap bubble [41], exploit an NKA which stabilizes cell volume against osmotic forces that drive water in by actively pumping Na^+ out and K^+ in. This mechanism indirectly establishes a negative membrane potential that moves Cl^- out of the cell making space for the impermeant molecules.
In synthesis, the NKA has the role of "nulling out" the effect of the impermeant molecules X, which have a net negative charge (z is in the range -2 to -0.7 [39]).

Therefore, both hydrostatic and osmotic pressures are involved in the control of fluid flow across the membrane. Since water is essentially incompressible, this flow directly affects cell volume change. This phenomenon is typically evident when cells are subjected to large osmotic shocks.
The assumption of a quasi-static theory is justified by the presence of a timescale

[2]Jacobus Van't Hoff was awarded of the first Nobel Prize in chemistry (1901) in recognition of his work on osmosis.

to reach the equilibrium of water of the order of tens to hundreds of milliseconds after a perturbation [48], while the typical timescales of ion relaxation after an osmotic shock is of the order of a few minutes [48][49].

Essentially, the system described by the PLM behaves like a chemical equilibrium, governed by the law of mass-action that moves to minimize its energy and find equilibrium after perturbation. The comparison with a globally asymptotically stable point in a nonlinear dynamical system [50] is straightforward; here, the PLM can be seen as a dynamic steady state.

By looking at the typical values for the PLM parameters in mammalian cells (table 2.2), some approximations can be made:

- the pumping efficiency $\alpha_0 \sim 0.14$ allows to assume the limiting case of "infinite pumping" ($\alpha_0 \sim 0$) where all the anions are pumped outside and the only ions inside the cell are the counterions of impermeant molecules.

- The osmotic pressure is balanced at the plasma membrane due to the difference of at least three orders of magnitude between hydrostatic and osmotic pressure; thus, the pressure difference (ΔP) affects cell shape but is not relevant in determining its volume.

- the density on ions outside the cell, n_0, and the one of impermeant molecules, x, are comparable ($\sim$ 120 mMol).

Combining these observations with equation 2.1, 2.2 and 2.3 it is possible to derive an expression for the volume as a function of molecules and ions number (see Appendix B for the complete derivation):

$$V = R + \frac{(z+1) \cdot X}{2n_0} \tag{2.4}$$

where R stands for the dry volume.

Therefore, there is a linear relation between volume and the impermeant molecules. What is left undefined is the specification of the contribution of different molecules (proteins, amino-acids and other metabolites) both to the volume and to the dry mass. Proteins represent 40-50% of the cell dry mass [38] [10] while metabolites and their counterions constitute most of the wet volume of the cell (78% of the total wet volume [38] [10]). It is worth noticing that the most abundant amino-acid, glutamate [38](see figure 2.3(b)), play a negligible role in building up proteins, suggesting the existence of amino-acids that can serve as regulators for other mechanisms, such as size homeostasis.

Overall, equation 2.4 suggests that the linear scaling between volume and proteins, already well established [51], is an indirect consequence of the linear scaling between proteins and metabolites (mainly amino-acids). This same behaviour is expected for nuclear concentration based on the observation of a fixed NC ratio [5]. In our study, these scaling of the nuclear volume with the metabolites content will be fundamental to analyze the dependence of the nuclear tension on the difference in the hydrostatic pressure at the NE.

However, a complete description of the scaling of the volume requires the understanding of the variations in the concentration of molecules (proteins, ions, amino-acids) present inside the cell. This is the aim of the next section.

2.2.2 Stochastic growth model

In this section a stochastic model for gene expression inspired by Lin[21] is used to prove the linear scaling relation between proteins and small osmolytes number which comes from the exponential growth regime of the cell as a consequence of the enzymatic control of amino-acid production.

This model couples cell volume growth and gene transcription and translation to describe how the synthesis of proteins and the presence of free amino-acids is fundamental to regulate cell volume growth; in particular, following this model it is possible to identify a transition from exponential growth to linear growth of protein number and cell volume.
The most innovative aspect of this work stands in the analysis of protein and mRNA exponential growth as a dynamical process, with transcription and translation rates proportional to the cell volume, rather than a deterministic process, with constant rates proportional to the genome copy number(constant rate model)(see figure 2.4).

The starting phenomenon is what is known as the central dogma of molecular biology: the genetic content present in the DNA is translated into proteins thanks to the mediation of the RNA. Because mRNA levels determine the rate of protein synthesis, the number of proteins per cell depends on the number of mRNAs, which in turn may depend on the number of active genes. In principle, a realistic stochastic model should include any process that indirectly affects the rates of gene expression and potentially randomizes protein concentrations. However, most models implicitly include all other processes in effective rate constants [52].

The model follows the basic idea of TASEP equations (totally asymmetric simple exclusion process) to describe how RNA polymerases (RNAPs) attach to genes in the transcription phase and result in mRNAs molecules and how ribosomes use this mRNA to obtain proteins. DNA and mRNA represent the substrates for

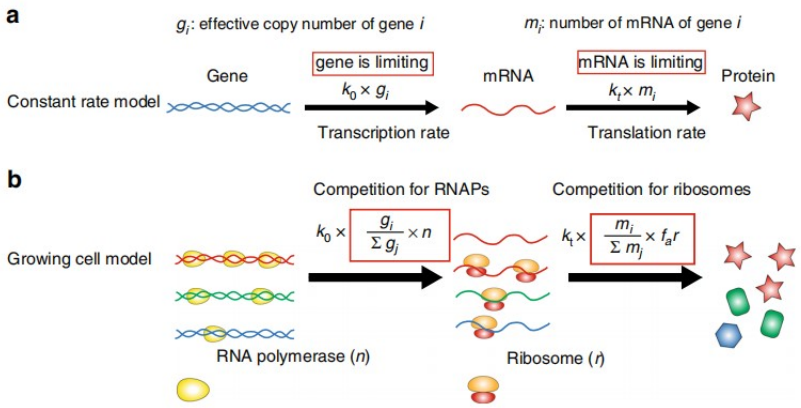

Figure 2.4: Schematic representation of a constant rate model (a) and a dynamical model with transcription and translation rates proportional to the cell volume (b). Adapted from Lin[21].

ribosomes and RNAPs. Assuming the number of ribosomes as the limiting factor in translation and the number of RNAPs as the limiting factor in transcription, different regimes for mRNA and protein synthesis can be identified based on the level of saturation respectively of DNA by RNAPs and mRNAs by ribosomes.

This process can be summarised in the following equations:

$$\dot{M}_i = \begin{cases} k_0 \cdot \phi_i \cdot p_r - \frac{M_i}{\tau_m}, & if \quad p_r \leq p_r^* \\ k_0 \cdot g_i \cdot p_r^{max} - \frac{M_i}{\tau_m}, & if \quad p_r \geq p_r^* \end{cases} \tag{2.5}$$

$$\dot{P}_i = \begin{cases} k_t \cdot \frac{M_i}{\sum_i M_i} \cdot r - \frac{P_i}{\tau_p}, & if \quad r \leq r^* \\ k_t \cdot m_i \cdot r^{max} - \frac{P_i}{\tau_p}, & if \quad r \geq r^* \end{cases} \tag{2.6}$$

where M, P, r, p_r represents the numbers of mRNAs, proteins, ribosomes and RNA polymerases; the pedex i stands for the gene i; k_0 and k_t characterize the transcription/translation rate of a single RNAP/ribosome and are constants; τ_m and τ_p represent the degradation rate of mRNAs and proteins; $\phi_i = \frac{g_i}{\sum_i g_i}$ and $\frac{M_i}{\sum_i M_i}$ are the fraction of substrates (DNA and mRNA) coding for product of type i, which can be seen as probabilities of attachment.

Here p_r^{max} e r^{max} are the maximum number of RNAPs that a single gene can hold and the maximum number of ribosomes above which mRNA starts to be saturated. They can be computed by imposing continuity of the production rate:

$$\phi_i \cdot p_r^{max} = g_i \cdot p_r^* \quad \rightarrow \quad p_r^* = \sum_i P_i \cdot p_r^{max} \tag{2.7}$$

$$\frac{M_i}{\sum_i M_i} \cdot r^{max} = M_i \cdot r^* \quad \rightarrow \quad r^* = \sum_i M_i \cdot r^{max} \tag{2.8}$$

Three regimes can be identified:

- Neither DNA nor mRNA is saturated
- Only DNA is saturated; the saturation of DNA precedes that of mRNAs, which number initially increases with the number of RNAPs while the number of genes remains constant.
- Both DNA and mRNA are saturated

An important approximation can be made on the mRNA: since τ_m has been found to be at least one order of magnitude smaller than τ_p in yeast, bacteria and mammalian cells [38], a quasi-static approximation, where $\dot{M}_i \sim 0$ during growth can be assumed (i.e. the number of mRNAs of type i adjusts instantaneously to the number of RNAPs). In the non saturated regime this leads to the following expression :

$$M_i = k_0 \cdot \tau_m \cdot \phi_i \cdot p_r \tag{2.9}$$

Coming to the amino-acids production, their production rate can be related to the number of enzymes catalyzing their biosynthesis, using a linear process by assuming that the nutrients necessary for the synthesis are in excess:

$$\dot{A} = k_{cat} \cdot e - l_p \cdot P_{tot} \tag{2.10}$$

where k_{cat} is the rate of catalysis and e is the number of enzymes. The second term represents the consumption of amino-acids to form proteins, with $P_{tot} = \sum_i P_i$. The transport of amino-acid through the plasma membrane is neglected.

2.2.3 Volume Scaling

Combining the Pump-Leak model, the growth model and the amino-acid biosynthesis model the following results can be understood:

- as long as mRNAs are not saturated (i.e., $r < r^*$) all the protein numbers scale with the number of ribosomes;
- the autocatalytic nature of ribosomes makes their number grows exponentially, i.e $r = r_0 \cdot e^{k_r \cdot t}$, with k_r the effective rate of ribosome formation;
- ribosomes exponential growth coupled to equation 2.10 results in the scaling of amino-acids and total protein content with the number of ribosomes with an initial exponential growth followed by saturation in the regime where both DNA and mRNA are saturated.

An important result of this model is that volume will first grow exponentially (i.e. regime where DNA is either saturated or not but mRNA is not saturated) and then it will show a linear increase with time (i.e. both DNA and mRNA have reached saturation).

For what concern our work, the exponential growth of the proteins inside the cell and its nucleus, which is the physiological one, will be important when it comes to study the evolution in time of the cell size and the duration of the G1 phase (see Chapter 5).

Chapter 3

Nucleus deformations and nuclear tension

The volume increase during the cell cycle is accompanied by organelles growth in response to the greater need for their functions. Among organelles, the nucleus holds a relevant role because of its primary function as a DNA container as well as due to its relatively simple geometry, which has made it the best candidate organelle for scaling studies [53].
Already suggested in 1921 by Champy and Carleton [54], the correlation between the shape of several types of animal cells and the shape of their nuclei has driven attention to the relation between cell size and nucleus size. However, despite advances in microscopy and other imaging techniques, the mechanism that allows the nucleus to maintain a specific scaling with cell size is still unclear.

The classical idea is based on considering the DNA content as a direct ruler for the volume of the nucleus (nucleoskeletal theory) and, as a consequence, for the cell volume [55] [56]. Nonetheless, this theory presents some flaws; for instance, it fails in explaining the presence of the same amount of DNA in different tissues in a given organism but with a variation in the nuclear size.

On the contrary, several studies have pointed out the need for a fixed NC ratio (i.e. even if the volume of the cell keeps growing, the nuclear to cellular volume ratio remains constant) to preserve the correct function of the cell [55]; indeed, anomalies of this ratio have been noticed in certain types of cancers [57], in certain protein mutations [58] [59] and its control has been suggested as a parameter to trigger cell cycle progression [60] [61].

A mathematical model (the "nested" Pump-Leak model) that treats the cell and the nucleus as two nested osmometers will be presented in the first section of this

chapter as a possible way to shed light on this debate following the same principles of the Pump-Leak model described in Chapter 2.

The mechanisms that determine the shape of the nucleus are an interesting subject to study. Different cells show a wide variety of nuclear shapes and sizes associated with different cell states, functions as well as pathological conditions, like genetic disorders, ageing, muscular dystrophy, dilated cardiomyopathy, and cancer progression [62] [40].
Two main hypotheses have been suggested to explain the origins of changes in nuclear shape: the alteration of the rigidity of the nucleus, i.e. change in the tension at the NE [63]; chromatin reorganization and consequent effect on gene expression [53].

Interestingly, an important change in the shape of the nucleus has been proven to be fundamental for the G1 to S transition. The flattening of the nucleus at this specific phase of the cell cycle is a consequence of the tension at the NE and may trigger transcriptional effects that promote cell cycle progression [35]. The origin of this tension is still unclear; what has been observed is that in normal cells the perinuclear actin cap filaments activate the response of myosin II and trigger the flattening of the nucleus. However, cells treated with an inhibitor of myosin II (blebbistatin) still present the correct G1/S transition if mechanically constrained [35].

In analogy with what has been observed in the case of cell migration [31], a key role is played by nuclear folds. Indeed, confinement of cells beyond a threshold height (defined by the size of the cell nucleus) causes an increase in the nuclear membrane tension and its unfolding, thus altering both volume and surface of the nucleus: the volume undergoes an abrupt decrease, while the surface augments [54]. Being the content of the nucleoplasm incompressible, this volume decrease is due to a water flux outward of the nucleus.
Interestingly, these wrinkles easily reform when the confinement is released (see figure 3.1(c)).
The stretch of nuclear folds triggers the release of calcium (Ca^{2+}) and cytosolic phospholipase A2 (cPLA2) with the inner nuclear membrane (INM), which may be a crucial factor to understand the mechanosensing properties of the nucleus [64] [35] (see figure 3.2 and 3.1(a)).

Based on these hypotheses, this section of the report is devoted to the derivation of the analytical expression for the tension at the NE. The result is obtained by combining the aforementioned nested Pump-Leak model with Laplace's law [66] to impose the balance of the osmotic and hydrostatic pressure at NE. A key factor is the assumption of a non-linear elastic model to describe the NE whose non-linearity

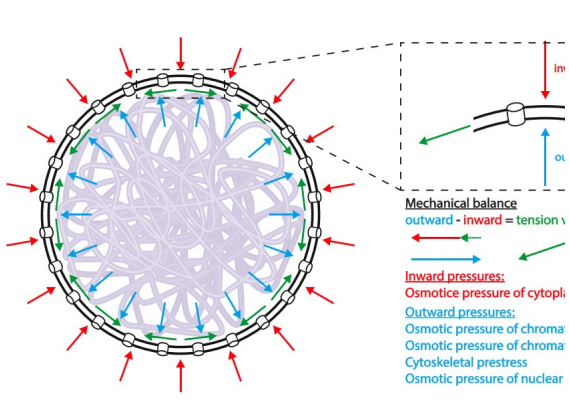

((a)) Force balance diagram for the NE. The inner and the outer membrane (the black concentric circle) intercalated by the nuclear pores, encapsulate the chromatin (light purple curve). The red and blue arrows stand respectively for the inward and outward components of the pressure exercised on the NE. The green arrows represent the response of the nuclear tension, the additional inward force to maintain the balance of mechanical forces. Adapted from Safran[63].

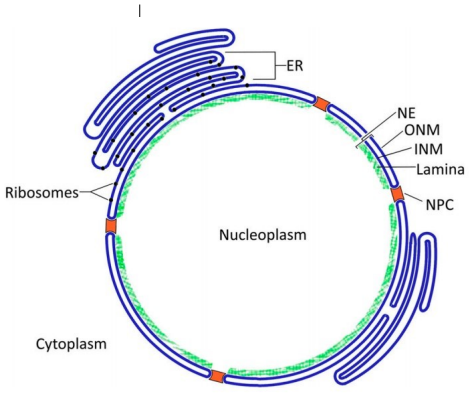

((b)) Structure of the nucleus. The nuclear envelope (NE) is composed of two membranes, the inner nuclear membrane(INM) and the outer nuclear membrane(ONM). The latter is connected to the endoplasmatic reticulum (ER), a characteristic which may play a crucial role in the process of nuclear growth and division. Below the INM there is a layer of lamina. The nucleoplasm can exchange material with the cytoplasm thanks to the existence of nuclear pores complex (NPC) on the NE. Adapted from Huber[65].

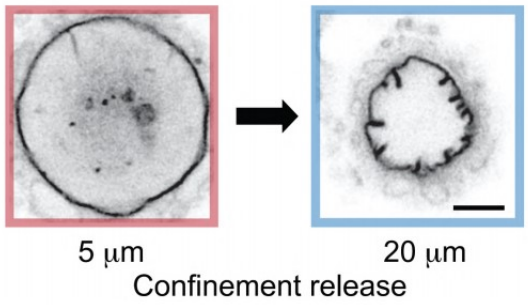

((c)) Effect of confinement on nuclear folds in *Hela* cell. Adapted from Lomakin[31].

Figure 3.1: Structure of the nucleus and its folds.

is justified by the presence of the nuclear folds. The tension γ is analyzed as a function of the control parameter h, the height of the confinement, and compared with numerical results presented in Rollin [10].

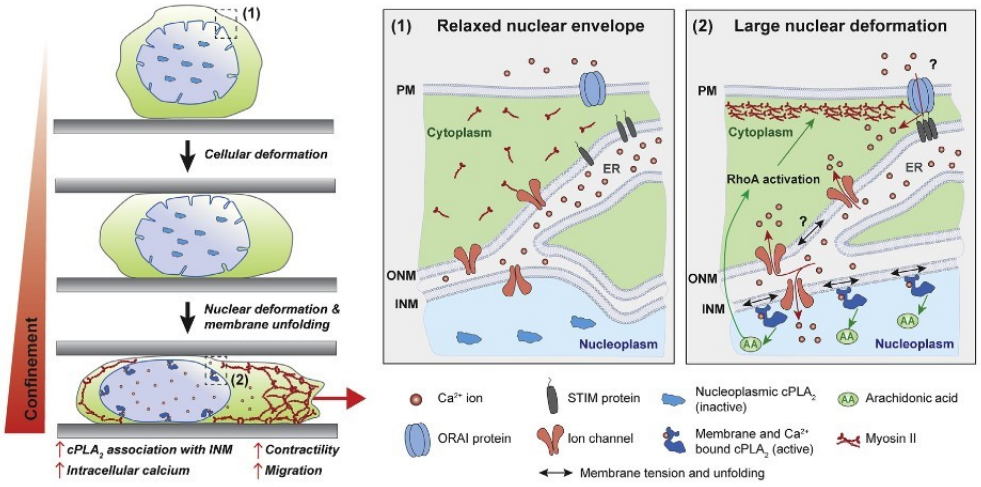

Figure 3.2: The nucleus acts as a mechano-sensor of confinement. Confinement under a critical threshold leads to increase nuclear tension and NE unfolding. In the unconfined state (1) the nuclear membrane is relaxed and under low tension; under strong confinement (2), the nucleus is deformed, the nuclear membrane is unfolded and the release on ions Ca^{2+} is activated with consequent cPLA2 production. STIM and ORAI proteins are molecules that allow the nuclear membrane to sense the level of Ca^{2+} and adapt to it the function of nuclear pores. Adapted from Long[64].

3.1 Nested Pump-Leak model

Motivated by the peculiar behaviour of the nucleus under compression and its relation with the G1/S transition, the simple Pump-Leak model presented in the previous chapter can be integrated by adding a new set of non-linear coupled equations related to the nucleus to predict how nuclear osmolytes and the tension at the NE evolves at different confinement heights. The result is the following system of equations which defines the nested Pump-Leak model:

$$\begin{cases} n_c^+ - n_c^- - z_a \cdot a_c - z_p \cdot p_c = 0 \\ n_c^+ + n_c^- + p_c + a_c - 2n_0 = \frac{\Delta\pi_c}{kT} = \frac{\Delta P_c}{kT} \sim 0 \\ n_c^+ \cdot n_c^- = \alpha_0 n_0^2 \\ n_n^+ - n_n^- - z_a \cdot a_n - z_p \cdot p_n = 0 \\ n_n^+ + n_n^- + p_n + a_n - q - 2n_0 - \frac{\Delta P_n}{kT} = 0 \\ n_n^+ \cdot n_n^- = \alpha_0 n_0^2 \end{cases} \tag{3.1}$$

where the index c and n refer respectively to the cytoplasm and to the nucleus. The symbols used have the same meaning as in section 1 with the additional term

q which represents the chromatin density inside the nucleus (see Appendix A).

To simplify the calculation some approximations can be made:

- the cytoplasm and the nucleoplasm can be considered ideal solutions; indeed, even if the cytoplasm and the nucleoplasm are crowded [67] [68], the presence of small osmolytes as the majority of free osmolytes allows to neglect steric and short range attractive interactions. Moreover, the electrostatic effect, which affects the spatial organization of charged molecules by attracting ions with opposite signs close to each other, is not significant as well; this choice can be justified by the general absence inside cells of phase transitions, which would be the signature of the impact of this polarization if it were relevant.
- The dry volume R, which plays the role of an excluded volume, is neglected. This assumption is aimed to simplify the calculations and does not affect the general result since R can be easily added afterwards.
- The formulas are derived in the particular case of z_p=z_a=1, justified by the estimation of Rollin [10].
- Only monovalent ions are considered; this approximation can be justified by the presence of multivalent ions, such as calcium and magnesium, only in the micromolar concentration range.

Following the same reasoning presented previously, an equation both for the cell volume, V_c, and for the nuclear volume, V_n, can be derived. However, an important difference must be taken into account: in the case of V_c the hydrostatic pressure ΔP does not play a central role in defining the volume since it is three orders of magnitude smaller than the osmotic pressure outside the plasma membrane π_0; on the contrary, ΔP is crucial when it comes to the nuclear volume if the nucleus is under strong nuclear envelope stretched.
In the following, the confinement height h will be the control parameter to identify the magnitude of the tension γ exerted at the NE.
As a consequence, it is possible to identify a unique equation for V_c (from equation 2.4) and two different equations for V_n depending on the strength of the nuclear tension γ :

$$V_c = \frac{2Pc + 2Ac}{2n_0} \tag{3.2}$$

$$V_n = \begin{cases} \frac{2Pn+2An+Q}{2n_0+\frac{\Delta P}{kT}} & \text{if the nucleus is under strong confinement} \\ \\ \frac{2Pn+2An+Q}{2n_0} & \text{if the nucleus is free from any confinement} \end{cases} \tag{3.3}$$

In addition to equations 3.1 and equations 3.2, 3.3, the condition on the potential at the nuclear/plasma membrane, which must equate the entropy contribution in the chemical potential, leads to the equality:

$$a_n \cdot (n_n^+)^{z_a} = a_c \cdot (n_c^+)^{z_a} \tag{3.4}$$

which under the previous assumption of z_a=1 reduces to:

$$a_n \cdot n_n^+ = a_c \cdot n_c^+ \tag{3.5}$$

The effect of a tension γ that acts on the nucleus can be understood in terms of fluxes of metabolites between the nucleus and the cytoplasm aimed to balance ΔP with $\Delta\pi$. Indeed, by looking at the equation for V_n 3.3, it is evident that there are three main classes of molecules which control the pressure balance: chromatin, proteins and metabolites.
Chromatin only plays an indirect role in nuclear volume through its counterions, since its translational entropy is vanishing, and introduces an asymmetry in the equations due to the formation of a potential at the NE related to the unbalanced ions. Moreover, its contribution to the osmotic pressure is typically one order of magnitude smaller than the one of proteins and other metabolites, making it negligible [63].
Proteins are considered as trapped in the nucleus; however, the ratio of the protein trapped on the total amount of cellular protein is about 0.5 (i.e. $\phi = \frac{P_n}{P_c+P_n} \sim 0.5$) since stuck inside the nucleus there are only the proteins with a mass above the critical value of 30-60 kDa, the maximum which allows to cross nuclear pores [38].
Metabolites, instead, are permeable to the NE but not to the plasma membrane. As a consequence, most of the volume of the nucleus depends on the presence of a large pool of metabolites which, differently from the number of chromatin counterions, grows with cell size and leads to the dilution of these counterions.

Taking into account this information, the study of the tension requires the understanding of the variation of the number of metabolites inside the nucleus and, as a consequence, of the nuclear volume.

Here we will derive the analytical expression for the number of metabolites A_n in the nucleus in three different regimes:

1. ΔP=0, no hydrostatic pressure, meaning that the nucleus is not under compression and the equation for A_n comes from the simple balance of the NC ratio.

2. $\frac{\Delta P}{2n_0kT} \to 0$, condition with biological consistency where the hydrostatic pressure

at the NE is small but it is still relevant thanks to the role of the lamina[1] in the nuclear membrane, absent in the plasma membrane (see figure 3.1(b) for a description of the structure of the nucleus). Indeed, the elastic properties of the lamina lower by two orders of magnitude with respect to the cytoplasm the typical hydrostatic pressure difference relevant for mechanical effects; moreover, lamina can preserve stress for a long time, contrary to cortical actin, because of its low turnover rate [69] [70].

3. $\Delta P \to \infty$, a regime that is not possible to observe in nature since it would lead to a drastic decrease in the cellular volume. In fact, since ΔP must balance $\Delta\pi$ and $\Delta\pi = \frac{N_n}{V_n} - 2n_0$, with N_n the total number of molecules inside the nucleus, higher ΔP implies $V_n \to 0$. Apart from its unlikelihood, this regime is an interesting way to check that the behaviour expected from this study is the correct one.

From the system of equations 3.1 it is possible to obtain the following expressions for the ionic concentrations:

$$\begin{cases} n_c^- = 0 \\ n_c^+ = p_c + a_c \\ n_0 = p_c + a_c \\ n_n^- = 0 \\ n_n^+ = p_n + a_n + q \\ n_0 = p_n + a_n + \frac{q}{2} + \frac{\Delta P}{2kT} \end{cases} \tag{3.6}$$

An expression for n_c^+ and n_n^+ in terms of n_0 can be easily deduced:

$$\begin{cases} n_c^+ = n_0 \\ n_n^+ = n_0 + \frac{q}{2} + \frac{\Delta P}{2kT} \end{cases} \tag{3.7}$$

Substituting expression 3.7 into equation 2.10 and writing in terms of numbers of molecules instead of concentrations, a general equation as starting point for the

[1]The nuclear lamina is a complex of intermediate filaments and membrane-associated proteins. It can be classified into three main types, A,B and C, depending on their DNA sequence and their biochemical activity. The inner nuclear membrane is mainly composed by lamin A and B [62] which has been observed to be the main element of response to mechanical stress.

three regimes listed above is directly obtained :

$$\frac{A_n}{V_n}(1+\frac{Q}{2n_0V_n}+\frac{\Delta P}{2n_0kT})=\frac{(A_0-A_n)}{V_c} \tag{3.8}$$

where the numbers of metabolites in the cytoplasm A_c have been obtained by subtracting the numbers of metabolites in the nucleus from the total amount of metabolites A_0 which is fixed.

3.1.1 $\Delta P = 0$

In this simple regime, the nuclear volume has the form

$$V_n=\frac{2P_n+2A_n+Q}{2n_0} \tag{3.9}$$

Inserting 3.9 into 3.8 and solving a second order equation in A_n, the result is

$$A_n=\frac{4P_n(A_0-P_c)-4QP_c-(2P_n+Q)^2+\sqrt{[4P_n(A_0-P_c)-4QP_c-(2P_n+Q)^2]^2-16(P_c+P_n)A_0(2P_n+Q)^2}}{8(P_n+P_c)}$$

The solution with the plus sign has been chosen in order to have a value for $A_n > 0$ which is the only realistic one.

3.1.2 $\frac{\Delta P}{2n_0kT} \to 0$

Proceeding as in the case $\Delta P = 0$, this time the equation to solve for A_n is a third-order equation:

$$\begin{aligned}&-8(\frac{\Delta P}{2n_0kT})A_n^3+[4(P_n+P_c)+8(\frac{\Delta P}{2n_0kT})(A_0+P_c-P_n-Q)]A_n^2-\\&-\{4[P_nA_0-P_c(P_n+Q)]-(2P_n+Q)^2-8(\frac{\Delta P}{2n_0kT})(P_c+A_0)(Q+P_n)\}A_n-(2P_n+Q)^2A_0=0\end{aligned} \tag{3.11}$$

The perturbation method is suitable to solve this equation (see Appendix C for the detailed calculation) since $\frac{\Delta P}{2n_0kT}$ appears as a perfect candidate to be used as a small parameter; indeed, by looking at the typical value found in a cell (see table 2.2), $2n_0kT$ is of order MPa while, with a physiological K of 25mN/m and length of micrometers, the hydrostatic pressure is of the order $\Delta P = 10^3$ Pa.

In this case A_n has the form:

$$A_n=A_n^0+(\frac{\Delta P}{2n_0kT})A_n^1 \tag{3.12}$$

where A_n^0 assumes the same form found in the case $\Delta P = 0$ (equation 3.10), while the first order term in $\frac{\Delta P}{2n_0kT}$ is

$$A_n^1 = \frac{8[A_n^{0\,3} - (A_0 + P_c - P_n - Q)A_n^{0\,2} + (P_c + A_0)(P_n + Q)A_n^0]}{8(P_n + P_c)A_n^0 + (2P_n + Q)^2 - 4[P_nA_0 - P_c(P_n + Q)]}$$

(3.13)

This complex formula can be simplified by exploiting a physiological argument: when the hydrostatic pressure is low, the metabolites tend to remain in the nucleus so their number will be much larger than the number of nuclear proteins and chromatin molecules. Moreover, the number of cytoplasmatic proteins is negligible with respect to A_n since, as stated above, it's almost equivalent to the value of P_n. From this consideration, equation 3.12 becomes

$$A_n = A_0\phi\Big\{\ 1 + \frac{\Delta P}{2n_0kT}\Big[\frac{2A_0\phi}{P_n}\Big(\phi - 1\Big)\Big]\Big\} \tag{3.14}$$

In this formula $\phi = \frac{P_n}{P_n+P_c}$ is the percentage of nuclear protein with respect to the total amount of protein inside the cell. This result is in good agreement with the first order term in $\frac{\Delta P}{2n_0kT}$ obtained solving directly the third order equation 3.11 in the limit $A_0 >> P_n, P_c, Q$ (the detailed calculation is given in Appendix C).

Another interesting limit to check this result is the one in which $Q = 0$, i.e. no chromatin counterions inside the nucleus. In this case equation 3.11 is reduced of one order and can be easily solved. The result gives

$$A_n = A_0\frac{P_n}{P_n + P_c}\Big[1 + \frac{\Delta P}{2n_0kT}\Big(\frac{2A_0P_n}{(P_n + P_c)^2} - 2\frac{A_0 + P_c}{P_n + P_c}\Big)\Big] \tag{3.15}$$

which is consistent with the result in 3.14 if also P_c is negligible with respect to A_0. It is interesting to notice that the meaning of the limit $Q = 0$ is evident if one looks at the second-order equation for A_n in the case $\Delta P = 0$. Under these conditions, the result coincides with the zero-order term in $\frac{\Delta P}{2n_0kT}$, i.e. $A_n = A_0\phi$, which in turn comes from the balance imposed by equation 3.5 in the absence of counterions, i.e. $\frac{A_n}{V_n} = \frac{A_c}{V_c}$.

3.1.3 $\Delta P \to \infty$

This last regime can be analyzed in an equivalent way to the case $\frac{\Delta P}{2n_0kT} \to 0$ yet considering $\frac{2n_0kT}{\Delta P} \to 0$. The equation for A_n is once again of third order;

nonetheless, the zero and first-order terms in $\frac{2n_0kT}{\Delta P}$ are vanishing and $A_n \sim (\frac{1}{\Delta P})^2$. The coefficient for $(\frac{2n_0kT}{\Delta P})^2$ coincides with equation 3.10, so that

$$A_n = (\frac{2n_0kT}{\Delta P})^2 \frac{4P_n(A_0 - P_c) - 4QP_c - (2P_n + Q)^2 + \sqrt{[4P_n(A_0 - P_c) - 4QP_c - (2P_n + Q)^2]^2 - 16(P_c + P_n)A_0(2P_n + Q)^2}}{8(P_n + P_c)}$$

The fact that the first non vanishing term is represented by the second order correction perfectly matches the expected behaviour for the flux of metabolites which, under strong pressure, tends to be directed outside of the nucleus.

The hydrostatic pressure is plotted as a function of h in figure 3.3 in the different regimes studied.
The biological meaningful case, i.e. $\frac{\Delta P}{2n_0kT} \to 0$ in figure 4.2(a), shows value of $\frac{\Delta P}{2n_0kT}$ in the order 10^{-3} as expected from the typical values listed in table 2.2.

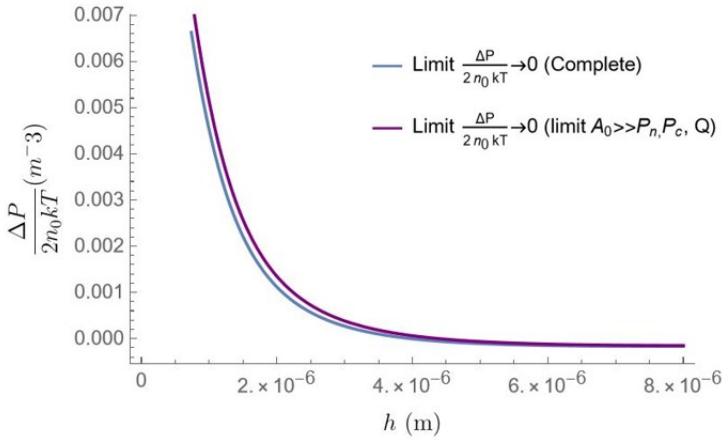

((a)) The hydrostatic pressure in the limit $\frac{\Delta P}{2n_0kT} \to 0$.

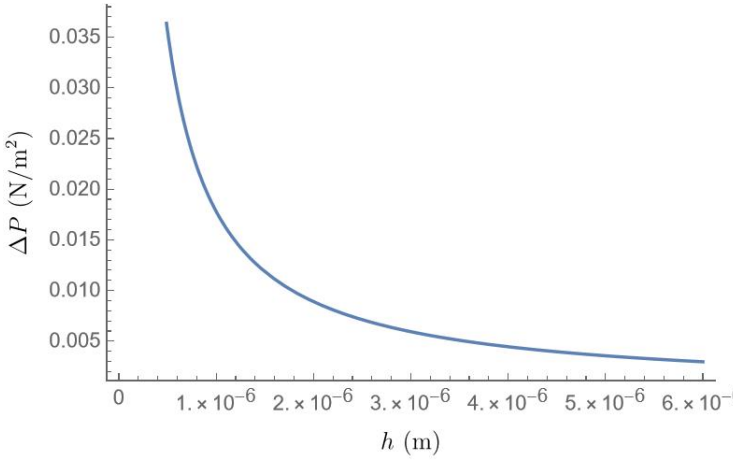

((b)) The hydrostatic pressure in the limit $\Delta P \to \infty$.

Figure 3.3: The hydrostatic pressure in different regimes as a function of the height of confinement. The values used for the different parameters can be found in table 3.1.

Parameter	Value
n_0	150 mMol
kT	4.1 pN.nm
K	1 mN/m
A_0	$1.3 * 10^{11}\ Mol * m^3$
P_c	$10^9\ Mol * m^3$
P_n	$10^9\ Mol * m^3$
Q	$2 * 10^9\ Mol * m^3$
S^*	$3.3 * 10^{-10} m^2$

Table 3.1: Values used for the plot of the analytical results.

Chapter 4

Nuclear tension

As mentioned previously, the cell cycle progression, in particular the G1/S transition, is characterized by an alteration of the nucleus which changes from an almost spherical into a flattened shape (see figure 4.1). The derivation of an analytical formula for the tension γ in the nucleus can help in finding the conditions that regulate this transition; in particular, it allows to study how γ behaves as a function of the control parameter h, the height of the confinement, therefore to identify a critical value of h starting from which γ has a non-null value.
The focus here will be on nuclei under uniaxial confinement, meaning that there is rotational invariance of the nucleus along one axis, and on the timescale of minutes, the timescale necessary to obtain a balance of the chemical potential of water at the nuclear envelope.
Two limiting regimes are interesting to study depending on the level of confinements:

1. spherical shape, i.e. $h \simeq R_0$ (radius of the nucleus in absence of compression), the nucleus is under weak confinement. The tension is buffered by the folds and the volume remains constant. In the ideal case of isotropic, three-dimensional growth of a spherical cell (in reality the shape of the nucleus is not perfectly spherical), since the sphere is the geometrical shape that minimizes the surface of any 3D objects, when h is decreased at constant volume then the surface must increase.

2. pancake shape, i.e. h small with respect to R_0, strong confinement. In this regime, the surface keeps increasing but the volume starts to decrease and it is no longer constant. The hypothesis to explain this volume loss is the existence of a "surface reservoir" represented by nuclear folds that stretch when h, and so γ, reaches a specific value, when the surface S reaches a critical value S^*.

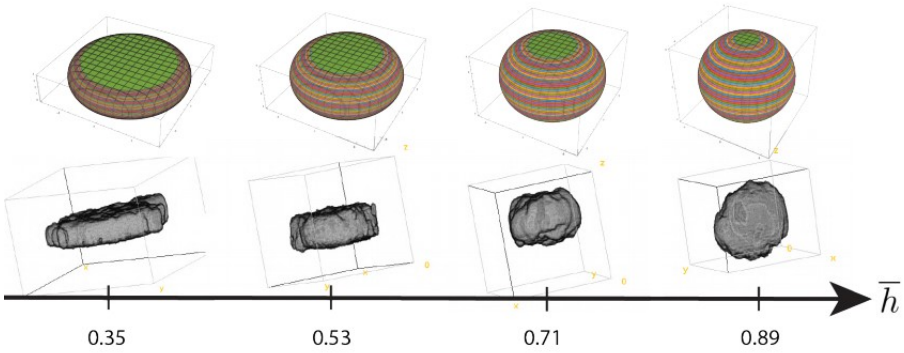

Figure 4.1: Evolution of the nucleus under confinement from a spherical to a pancake shape. Adapted from Rollin [10].

Making use of the equations obtained for the metabolites as a function of the hydrostatic pressure, here we will derive an analytical formula for the nuclear tension as a function of h in both regimes to check if and under which conditions the analytical results are in agreement with the numerical solution.
The computation is based on Laplace's law [66], which relates the pressure difference at the NE (ΔP) with the nuclear tension (γ) and the shape of the surface, i.e. its curvature. In its most general form:

$$\Delta P = 2\gamma(\frac{1}{R_1} + \frac{1}{R_2}) \tag{4.1}$$

where R_1 and R_2 stand for the principal radii of curvature. Under the assumption of elastic behaviour for the NE, the tension γ is well described by the following function:

$$\gamma = \begin{cases} K(\frac{S}{S^*} - 1) & if \quad S > S^* \\ 0 & if \quad S < S^* \end{cases} \tag{4.2}$$

with a stretching modulus K and a critical surface area S^* above which NE folds are stretched. Beginning from this equation and substituting the right expression for S in terms of the volume V_n, an equation for ΔP, and therefore for γ, is derived. Nevertheless, the result is expected to be different in the two different regimes since in the case of a sphere $S \sim V^{\frac{2}{3}}$ with a sub-linear scaling, while in the pancake case, the scaling is linear, $V \sim S \cdot h$.
Hence, for the same increment of volume, the tension will increase more in the latter case.

4.1 Spherical shape

Being the most common shape for nuclei [71], the spherical geometry represents a good starting point for our analysis. In this regime, we choose as radii of curvature simply the initial radius before compression, R_0. With this choice, Laplace's law becomes:

$$\Delta P = \frac{2\gamma}{R_0} \tag{4.3}$$

where R_0 is related to the volume by $V_n = \frac{4\pi R_0^3}{3}$. Using the general formula to compute the surface of a sphere, $S = 4\pi R_0^2$, the constitutive equation for γ assumes the form:

$$\gamma = K(\frac{4\pi(\frac{3V_n}{4\pi})^{\frac{2}{3}}}{S^*} - 1) \tag{4.4}$$

Putting together these two equations, we have an expression for the hydrostatic pressure as a function of the volume:

$$\Delta P = 2K\left[\frac{4\pi}{S^*}(\frac{3}{4\pi}V_n)^{\frac{1}{3}} - (\frac{3}{4\pi}V_n)^{-\frac{1}{3}}\right] \tag{4.5}$$

As expected, the relationship is non-linear.

To proceed with the calculation, we take the limit in which $\frac{\Delta P}{2n_0kT} \to 0$ since it is the most relevant one. In this regime it is possible to substitute the volume in equation 4.5 with:

$$V_n = \frac{2A_n + 2P_n + Q}{2n_0}(1 - \frac{\Delta P}{2n_0kT}) \tag{4.6}$$

where the factor $(1 - \frac{\Delta P}{2n_0kT})$ comes from a Taylor expansion at the first order of the denominator in equation 3.3 for V_n.
A_n has the expression found in the previous section (see equation 3.12).
Combining these results and again applying a Taylor expansion for the power of $(1 - \frac{\Delta P}{2n_0kT})$ keeping only terms of order one, a general expression for ΔP can be obtained:

$$\Delta P = \frac{2K\left[(\frac{4\pi}{S^*})(\frac{3}{4\pi}\frac{2P_n+2A_n^0+Q}{2n_0})^{\frac{2}{3}} - 1\right]}{(\frac{3}{4\pi}\frac{2P_n+2A_n^0+Q}{2n0})^{\frac{1}{3}}\left[1 - \frac{2K}{3n_0kT}(\frac{3}{4\pi}\frac{2P_n+2A_n^0+Q}{2n0})^{\frac{1}{3}}\frac{4\pi}{S^*}(\frac{2A_n^1}{2P_n+2A_n^0+Q} - 1)\right]} \tag{4.7}$$

This formula can be simplified in the regime $A_0 >> P_n, P_c, Q$, which is the case in the approximation used above of small $\frac{\Delta P}{2n_0kT}$. Therefore, we have:

$$\Delta P = \frac{2K\left[(\frac{4\pi}{S^*})(\frac{3}{4\pi}\frac{A_0\phi}{n_0})^{\frac{2}{3}} - 1\right]}{(\frac{3}{4\pi}\frac{A_0\phi}{n0})^{\frac{1}{3}}\left\{1 - \frac{2K}{3n_0kT}(\frac{4\pi}{S^*})(\frac{3}{4\pi}\frac{A_0\phi}{n0})^{\frac{1}{3}}\left[(\frac{2A_0\phi}{P_n})(\phi - 1) - 1\right]\right\}} \tag{4.8}$$

The equation for ΔP assumes a general form that can be deduced from the following calculation.
From Laplace's law we know the relation between the hydrostatic pressure and the radius of the nucleus R:

$$\Delta P = 2K\Big(\frac{R}{R^*} - \frac{1}{R}\Big) \tag{4.9}$$

where R^* is the radius related to the critical surface S^*.
The value of R can be deduced from the volume:

$$V_n = \begin{cases} \Big(\frac{2P_n+2A_n^0+Q}{2n_0}\Big)\Big[1+\frac{\Delta P}{2n_0kT}\big(\frac{A_n^1}{2P_n+2A_n^0+Q}-1\big)\Big] & \text{general case} \\ \\ \frac{A_0\phi}{n_0}\Big[1+\frac{\Delta P}{2n_0kT}\Big(\frac{2A_0\phi}{P_n}(\phi-1)-1\Big)\Big] & \text{if } A_0 >> P_n, P_c, Q \end{cases} \tag{4.10}$$

that can be expressed in the form:

$$V_n = V_n^0(1+\epsilon c) \tag{4.11}$$

where $\epsilon = \frac{\Delta P}{2n_0kT}$ and:

$$c = \begin{cases} \frac{A_n^1}{2P_n+2A_n^0+Q} - 1 & \text{general case} \\ \\ \frac{2A_0\phi}{P_n}(\phi-1)-1 & \text{if } A_0 >> P_n, P_c, Q \end{cases} \tag{4.12}$$

From this expression for the volume we can deduce a general form for the radius:

$$R = R_0(1+\frac{1}{3}\epsilon c) \tag{4.13}$$

Using this expression for R in Laplace law and keeping only first order terms in ϵ, we obtain:

$$\Delta P = \frac{\Delta P^0}{1-\frac{2KR_0c}{R^{*2}3n_0kT}} \tag{4.14}$$

Here ΔP^0 represents the hydrostatic pressure in the absence of confinement. Its value can be deduced from the previous equation:

$$\Delta P^0 = \begin{cases} \frac{2K\Big[(\frac{4\pi}{S^*})(\frac{3}{4\pi}\frac{2P_n+2A_n^0+Q}{2n_0})^{\frac{2}{3}}-1\Big]}{(\frac{3}{4\pi}\frac{2P_n+2A_n^0+Q}{2n0})^{\frac{1}{3}}} & \text{general case} \\ \\ \frac{2K\Big[(\frac{4\pi}{S^*})(\frac{3}{4\pi}\frac{A_0\phi}{n_0})^{\frac{2}{3}}-1\Big]}{(\frac{3}{4\pi}\frac{A_0\phi}{n0})^{\frac{1}{3}}} & \text{if } A_0 >> P_n, P_c, Q \end{cases} \tag{4.15}$$

Once we have an equation for the hydrostatic pressure, the analytic form of γ is straightforward from Laplace's law:

$$\gamma = \frac{\Delta P}{2} R_0 \tag{4.16}$$

which in the general case becomes

$$\gamma = \frac{1}{2}(\frac{3}{4\pi})^{\frac{1}{3}}(\frac{2A_n^0 + 2P_n + Q}{2n_0})^{\frac{1}{3}}\Delta P \tag{4.17}$$

and in the limit $A_0 >> P_n, P_c, Q$

$$\gamma = \frac{1}{2}(\frac{3}{4\pi})^{\frac{1}{3}}(\frac{A_0\phi}{n_0})^{\frac{1}{3}}\Delta P \tag{4.18}$$

where in both formulas ΔP has the form calculated before.

From formula 4.18 we can see that γ increases with the nuclear volume, which can be verified with a simple reasoning: the elastic equation relates the tension and the radius of the nucleus R, $\gamma \sim (\frac{R}{R^{*2}} - \frac{1}{R})$; the radius of the nucleus increases as the volume becomes bigger, making the first term going $\to \infty$ while the second term goes $\to 0$. Therefore, this result matches our prediction: a cell born bigger will have a higher nuclear tension than a cell with a smaller volume at birth and this will affect the length of the G1 phase (as we will see in the next chapter).

4.2 Pancake-like shape

The regime in which the tension affects the behaviour of the nucleus during growth is the one in which the nucleus tends to have a flat shape that we will call pancake shape. In this condition, we can use the following equation for the volume

$$V_n = \frac{h}{2} S_n \tag{4.19}$$

where S_n represents the contact surface of the squeezed nucleus[1]. The parameter h represents also the main radius of curvature so that Laplace's law takes the form

$$\Delta P = \frac{2\gamma}{h} \tag{4.20}$$

[1]In reality the nucleus is not in direct contact with the surface of confinement but it senses it through specific protein complexes that link both surfaces, such as the LINC complex; however, in our simple analysis we will neglect the mechanism that allows the nucleus to be in contact with the external surface.

Combining both formulas with the elastic equation for the tension, it is possible to derive an expression for V_n linear in ΔP

$$V_n = \frac{h}{2} S^* (\frac{h}{2K} \Delta P + 1) \tag{4.21}$$

In order to find the expression for ΔP, and, as a consequence, for γ, we work once again in the regime of small ΔP. By equating this formula for the volume with the same one exploited in the spherical case 4.6, the equation for ΔP becomes

$$\Delta P = \frac{2P_n + 2A_n^0 + Q - \alpha}{\frac{\alpha h}{2K} - \frac{1}{n_0 kT} A_n^1 + \frac{P_n}{n_0 kT} + \frac{A_n^0}{n_0 kT} + \frac{Q}{2n_0 kT}} \tag{4.22}$$

with $\alpha = n_0 h S^*$. In the limit $A_0 >> P_n, P_c, Q$, then this formula is simplified in

$$\Delta P = \frac{1 - \frac{\alpha}{2A_0\phi}}{\frac{1}{2n_o kT} - \frac{A_0\phi^2}{n_0 kTP_n} + \frac{A_0\phi}{n_0 kTP_n} + \frac{\alpha h}{4A_0\phi K}} \tag{4.23}$$

The tension can be obtained from Laplace's law, i.e. multiplying ΔP by $\frac{h}{2}$:

$$\gamma = \begin{cases} \frac{h}{2} \frac{2P_n + 2A_n^0 + Q - \alpha}{\frac{\alpha h}{2K} - \frac{1}{n_0 kT} A_n^1 + \frac{P_n}{n_0 kT} + \frac{A_n^0}{n_0 kT} + \frac{Q}{2n_0 kT}} & \text{general case} \\ \\ \frac{h}{2} \frac{1 - \frac{\alpha}{2A_0\phi}}{\frac{1}{2n_o kT} - \frac{A_0\phi^2}{n_0 kTP_n} + \frac{A_0\phi}{n_0 kTP_n} + \frac{\alpha h}{4A_0\phi K}} & \text{if } A_0 > P_n, P_c, Q \end{cases} \tag{4.24}$$

The analytical result compared to the numerical one is plotted in figure 4.2.
As expected, the analytical formula obtained in the regime $\frac{\Delta P}{2n_0 kT} \to 0$ is in good agreement with the numerical solution for a small value of γ. The plot in figure 4.2(a) and 4.2(c) displays a worse match between the analytical and the numerical result than the plot in figure 4.2(b) and 4.2(d); indeed, the first plots represent the simplified solution, the one in which the number of proteins (P_n and P_c) and the number of chromatin counterions (Q) is negligible with respect to A_0, while the second plots show the solution in the general case. The main difference in the two results resides in the critical value of h at which the tension starts to be positive and, once again, underlines the link between the fluxes of metabolites inward/outward of the nucleus and its response to mechanical stress. Indeed, a bigger number of metabolites inside the nucleus has the effect of increasing the critical value of h, which means, the tension is felt by the nucleus earlier since more molecules have to leave the nucleus to reestablish the balance between osmotic and

hydrostatic pressure.

This critical value of h is related to S^* as equations 4.22 and 4.23 show, where the parameter S^* appears in α, since the h critical is defined by the value of the height obtained from imposing that the numerator in equations 4.22 or 4.23 vanishes. The effect of an increase in S^* is a decrease in the value of h from which the tension starts to be positive due to the fact that S^* bigger implies that the NE can sustain a stronger confinement before being stretched and feeling the tension γ.

It is worth mentioning that the result gets better as the parameter K is decreased (figure 4.2(a) and 4.2(b) with K=1 mN/m show a better agreement with the numerical result than figure 4.2(c) and 4.2(d) where K=3 mN/m) since a smaller stretching modulus improves the approximation of a pancake shape (used to compute the volume as $V_n = \frac{h}{2} S_n$). Indeed, the smaller the stretching modules, the weaker the nuclear tension γ; since the spherical shape is the one that maximizes the surface tension, i.e. the tension at the NE, a small value of γ implies the presence of a shape far from the spherical one and close to a flat one.

Further checking of these formulas can be done taking the opposite limit for ΔP, i.e. $\Delta P \to \infty$. In this regime, the calculation follows the same steps seen up to now with the only difference that the small parameter in which the expansion can be made is $\frac{2n_0 kT}{\Delta P}$.
Since, as computed in the previous section, the number of metabolites is negligible in this limit, the volume assumes the form

$$V_n = \frac{2P_n + Q}{2n0} \Big(\frac{2n_0 kT}{\Delta P} \Big) \Big(1 - \frac{2n_o kT}{\Delta P} \Big) \tag{4.25}$$

The expression for the hydrostatic pressure is now

$$\Delta P = \frac{2n_0 kTK}{\alpha h} \Big(-\frac{\alpha}{2n_0 kT} + \sqrt{(\frac{\alpha}{2n_0 kT})^2 + (\frac{\alpha}{2n_0 kT})(2P_n + Q)} \Big) \tag{4.26}$$

which diverges as h decreases.
While the tension, which has a further factor h in the numerator, goes to a constant. This result can be understood since, as said before, the volume scales as $\frac{1}{\Delta P}$, so when $\Delta P \to \infty$ it is expected to vanish. If we consider the surface as a constant, $V_n \sim hS$ implies that $h \to 0$ and $\gamma =$ constant.

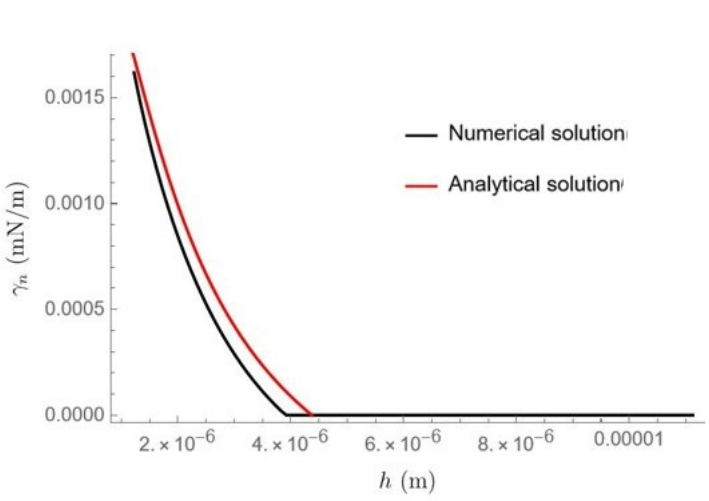

((a)) The tension in the limit $\frac{\Delta P}{2n_0kT} \to 0$ with $A_0 > P_n, P_c, Q$.

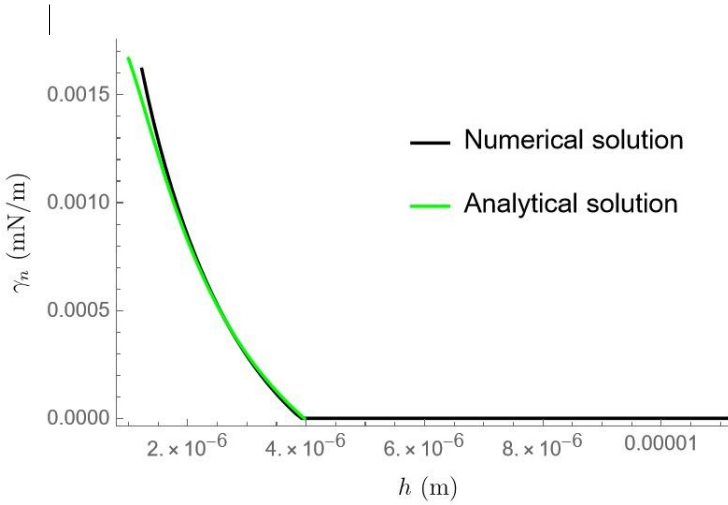

((b)) The tension in the limit $\frac{\Delta P}{2n_0kT} \to 0$ in the general case.

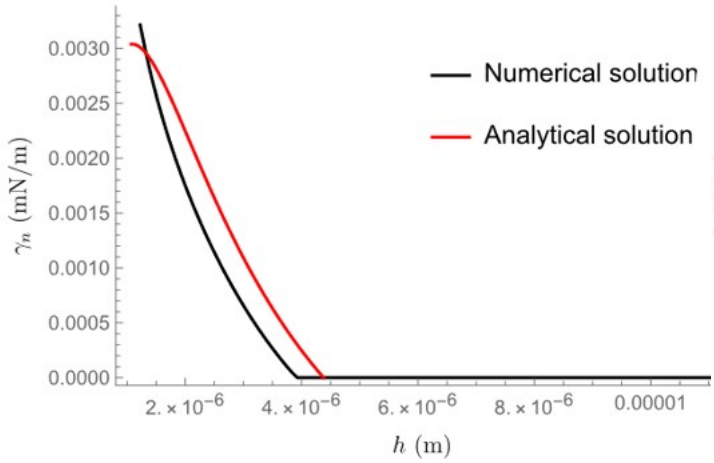

((c)) The tension in the limit $\frac{\Delta P}{2n_0kT} \to 0$ with $A_0 > P_n, P_c, Q$.

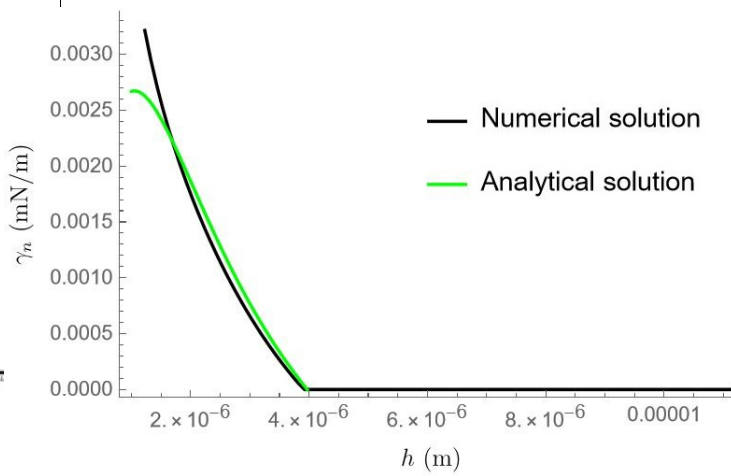

((d)) The tension in the limit $\frac{\Delta P}{2n_0kT} \to 0$ in the general case.

Figure 4.2: Comparison between the numerical and the analytical result for the tension as a function of h. The parameter K is fixed at a value of 1 mN/m in figure 4.2(a) and 4.2(b) and at the value of 3 mN/m in figure 4.2(c) and 4.2(d). The values used for the computation are listed in table 3.1.

The tension in the different regimes studied is plotted as a function of h in figure 4.3.

It should be pointed out that figure 4.3(a) shows the whole plot of the tension, in contrast with the result in figure 4.2. In the latter γ is plotted only in the range of values of h where the approximation $\frac{\Delta P}{2n_0kT} << 1$ is valid and the tension follows the expected behaviour, i.e. γ increases as h becomes smaller.

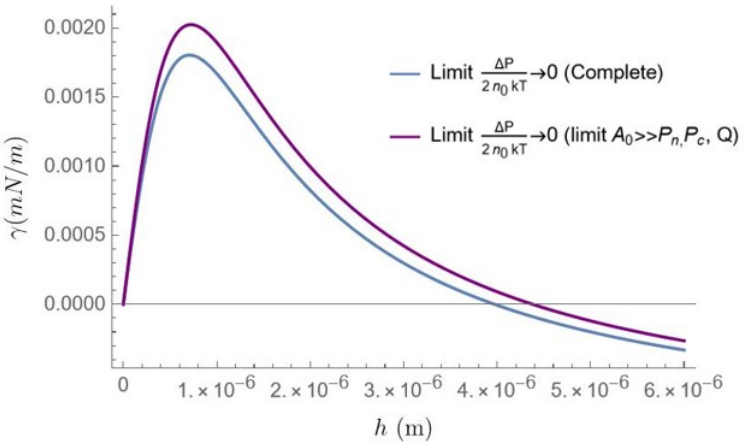

((a)) The tension in the limit $\frac{\Delta P}{2n_0kT} \to 0$ with $A_0 > P_n, P_c, Q$.

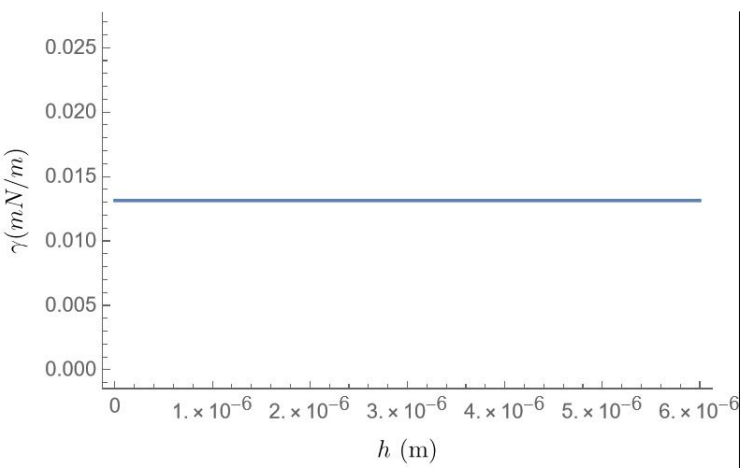

((b)) The tension in the limit $\Delta P \to \infty$ in the general case.

Figure 4.3: The tension in different regimes as a function of the height of confinement. The values used refers to table 3.1.

An interesting parameter that helps in understanding the mechanical response of the nucleus is the osmotic compressibility β [2].
The usual definition of compressibility in thermodynamics and fluid mechanics identifies β as the relative volume change to a variation in pressure; mathematically, it has the following expression:

$$\beta = -\frac{1}{V_n}\frac{\delta V_n}{\delta \pi_n} \tag{4.27}$$

where the minus sign ensures a negative correlation between volume and pressure. For simplicity we have computed the inverse of the compressibility, the bulk modulus $\kappa = -V_n \frac{\delta \pi_n}{\delta V_n}$.
Indeed, knowing that $\pi_n = \frac{(2A_n+2P_n+Q)kT}{V_n}$ and V_n has the form seen in equation

[2]Taking into account the condition of constant temperature assumed in this work, here we deal with isothermal compressibility.

4.6, with a fixed number of protein and chromatin counterions, the variation of the osmotic pressure with respect to the volume becomes:

$$\frac{\delta\pi_n}{\delta V_n} = -\frac{(2A_n + 2P_n + Q)kT}{V_n^2} + \frac{2}{V_n}kT\frac{\delta A_n}{\delta V_n} \tag{4.28}$$

In the regime where $A_0 >> P_n, P_c, Q$, the second factor in the above equation can be computed from the formula 3.14 by exploiting the chain rule:

$$\frac{\delta A_n}{\delta V_n} = \frac{\delta A_n}{\delta \frac{\Delta P}{2n_0 kT}} \frac{\delta \frac{\Delta P}{2n_0 kT}}{\delta V_n} \tag{4.29}$$

The final result gives the following formula for κ:

$$\kappa = \frac{2A_0\phi}{V_n}\left[1 + \frac{\Delta P}{2n_0kT}\frac{2A_0\phi}{P_n}(\phi - 1)\right]kT - 2n_0kT = \\ = \pi_{n0}\left[1 + \frac{2A_0\phi}{P_n}(\phi - 1)\frac{\Delta P}{2n_0kT}\right] - \pi_0 \tag{4.30}$$

where $\pi_{n0} = \frac{2A_0\phi}{V_n}kT$ is the nuclear osmotic pressure in absence of hydrostatic pressure and $\pi_0 = 2n_0kT$ is the cytoplasmic osmotic pressure (assuming osmotic equilibrium between the cytoplasm and the external environment, i.e. $\pi_c = \pi_0$).
An interesting information that can be derived from this calculation is the dependence of the compressibility on the content of the nucleoplasm, in agreement with the suggestions of previous works [72] [73].
Indeed, an increase in the nuclear metabolites, i.e. an increase in the hydrostatic pressure, is related to a higher value of κ, which means that in bigger cells the nuclear volume tends to be less sensitive to the change in osmotic pressure.
The order of magnitude reached by this parameter with the typical values found in a cell (see table 3.1) is of $10^2\frac{m^2}{N}$.

Chapter 5

Model of growth and G1 length

The results obtained so far are useful tools to analyze more in details how the mechanism that regulates the checkpoint between the G1 and the S phase of the cell cycle is related to the length of the G1 phase itself.

Long time ago, it was common to talk about 'Points of no return' rather than 'checkpoints'. Though, the word 'checkpoints' invokes both the idea of an event that cannot happen before the one in which you are presently engaged is complete and the fact that, once you have proceeded you cannot go back.
Between the different control points, the one that determines the G1/S transition seems to play a peculiar role; already in the '70 of the last century the G1 phase was known to be different with respect to the other two phases that precede mitosis, S and G2, since its duration is not a constant among different species but it's extremely variable [74]. This special characteristic of the G1 phase has led to a reconsideration of the definition of the cell cycle itself: the term 'cycle' reflects a regularly recurring process, which is suitable in the case of the S-G2-M progression, while it is not suitable for the G1 phase which appears as a randomly occurring event with a certain probability.

Recent theories suggest that at least two requirements are needed for the G1 exit: a size threshold and a minimal extension in G1. A transition point exists when one of the two types of cell size homeostasis mechanisms is limiting [75]. Therefore, the key parameters that can be observed to affect the cell size homeostasis are both growth rate and time [76]. Interestingly, recent experiments have shown that there is a relation between the decision to start the division and leave the G1 phase and the size of the nucleus of the cell in proliferating tissues: when the nucleus is compressed and reaches a minimal size, division can no longer occur since it would

imply damage of the DNA [6].

Supported by this observation, our study can be concluded with the calculation of the time spent in the G1 phase and an analysis of its dependence on the height of confinement h and the critical value of the tension γ_c to activate the G1/S transition.

The computation proceeds as follows:

- we start with the equation obtained in the previous section for the hydrostatic pressure;
- we substitute constant values for A_n, P_n, P_c with parameters that increase exponentially (choice motivated by the results for the scaling of the metabolites and the proteins with the cell volume obtained from the stochastic model for gene expression), i.e. $P_n = P_{n0}e^{k_r t}$, $P_c = P_{c0}e^{k_r t}$ and $A_n = A_{n0}e^{k_r t}$ with k_r the growth rate (assumed equal for all the molecules for the sake of simplicity, $k_r = 10^{-1}$ hours);
- once we have an expression for ΔP, the tension is found by multiplying it with $\frac{h}{2}$ (see figure 5.1);
- by imposing that at a specific critical value γ_c the G1 phase is arrested, the inverse of the formula for the critical tension gives the value of the duration of the G1 phase, t_1.

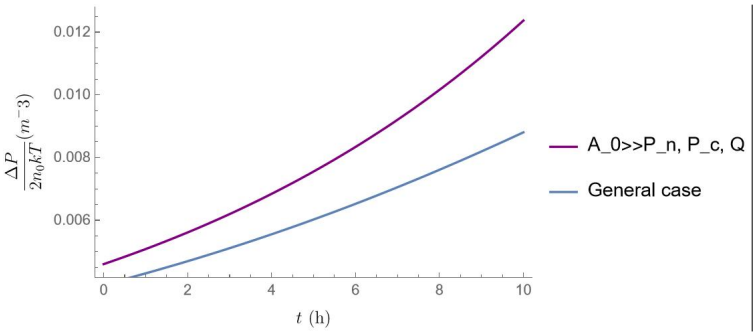

((a)) The hydrostatic pressure in the limit $\frac{\Delta P}{2n_0kT} \to 0$.

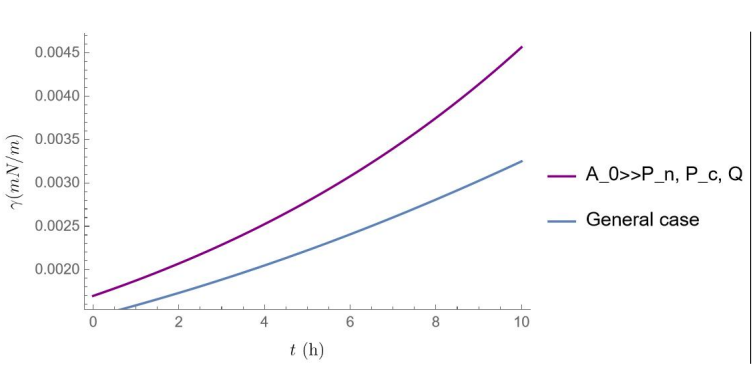

((b)) The nuclear tension in the limit $\frac{\Delta P}{2n_0kT} \to 0$.

Figure 5.1: The hydrostatic pressure and the tension in different regimes as a function of time.

It is interesting to notice that both the hydrostatic pressure and the nuclear tension grow faster in the case $A_0 >> P_n, P_c, Q$; indeed, in this limit, the dominant

contribution comes from the exponential increase in the number of metabolites, whereas in the general case the nucleoplasm has also constant chromatin counterions Q which do not increase over time.

The complexity of the expression makes it hard to compute an analytical equation for t_1. However, if we limit the calculation to the case $A_0 >> P_n, P_c, Q$, then t_1 has a close analytical form of the type

$$t_1 = \frac{1}{k_r}\left[\log\Big(\frac{\alpha}{2A_0\phi}\Big) + \log\Big\{\ 1 + \frac{\gamma_c}{hn_0kT}\left[1 + \frac{1}{K} + \frac{2A_0\phi}{P_n}(1-\phi)\right]\Big\}\ \right] \tag{5.1}$$

which has been obtained considering that in the biological relevant case $\gamma_c \to 0$. The results are shown in figure 5.1 and 5.2 where t_1 is plotted with respect to the value of h and of γ_c.

5.1 Comparison with the experiments

As expected from the experimental results, the duration of the G1 phase is extended in the case of low confinement, i.e. h large, since in this case the value of the tension is lower at the beginning of the G1 phase and it requires more time to reach the critical value γ_c for the transition.

The inverse is also true, which means a bigger value of γ_c at fixed h requires longer t_1.

Overall, despite the simplifications assumed, the general behaviour of t_1 is in good agreement with the one expected.

Indeed, figure 5.2(b) shows the evolution of the time in G1 if we fix $\gamma_c = 0.5\mu N/m$. This choice of the critical tension comes from the analysis of the plot in figure 5.2(a) where it is evident that, at fixed $h = 20\mu m$, γ_c in the range between 0 and $0.6\mu N/m$ is associated to a t_1 between 6 and 11 hours, which is the typical duration of the G1 phase observed in experiments.

A remarkable result is shown in figure 5.3 where the time in G1 is plotted as a function of the total volume of the cell $(V_n + V_c)$ at birth with a confinement of h=20μm. This plot can be compared to the experimental result obtained by Piel's team (see figure 2.2); indeed, in both figures it is evident that the time in the G1 phase decreases as the initial volume of the cell gets bigger. The plot is shown in a specific range for the initial volume (between 1000μm and 2700 μm)

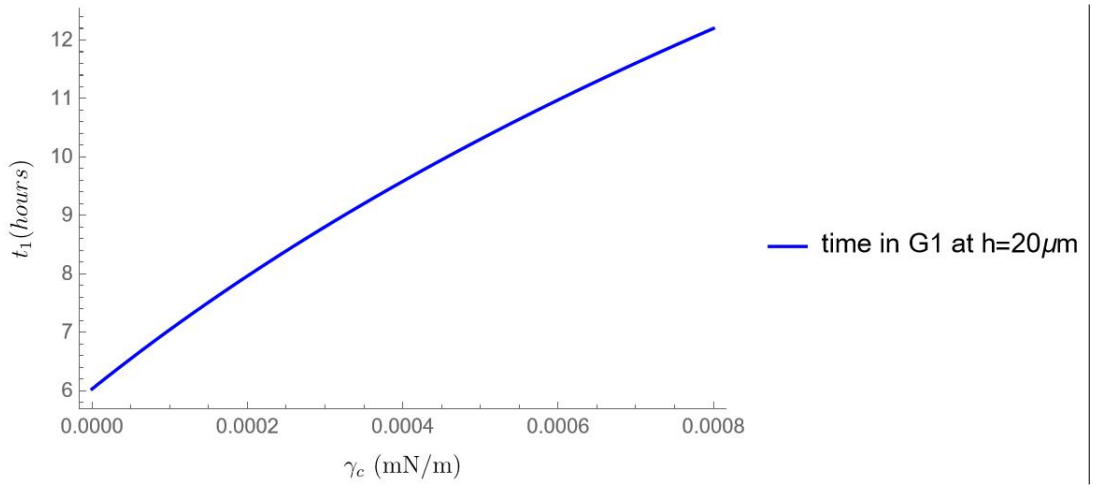

((a)) Time in G1 as function of γ_c. A bigger value of the critical tension requires more time for the cell to grow and reach the restriction point.

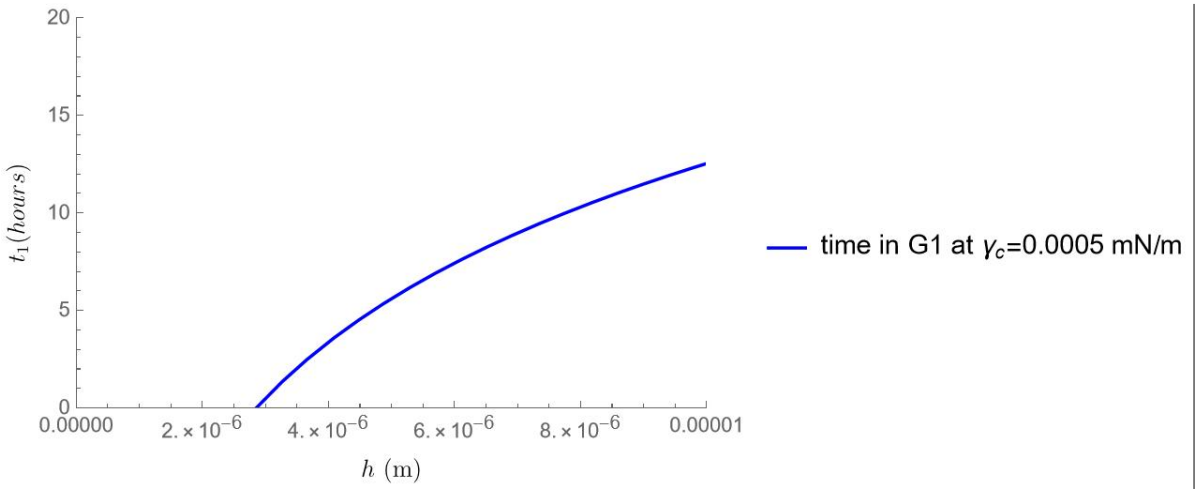

((b)) Time in G1 as a function of the height of confinement. Stronger confinement implies a shorter G1 phase. It is worth noticing that there is a critical value of h (h $\sim 3\mu m$ with our choice of parameters) below which the time becomes negative. This unrealistic result suggests that the confinement cannot go beyond a certain height because it would dramatically lead to a null volume of the nucleus.

Figure 5.2: Time spent in G1 as function of the parameters h and γ_c. The values used are listed in table 3.1.

since experimentally it has been observed that, when a threshold value for the confinement is reached, the time spent in the G1 phase no longer depends on the volume at birth but has a constant value ~ 6 hours (thin grey horizontal line in the plot).

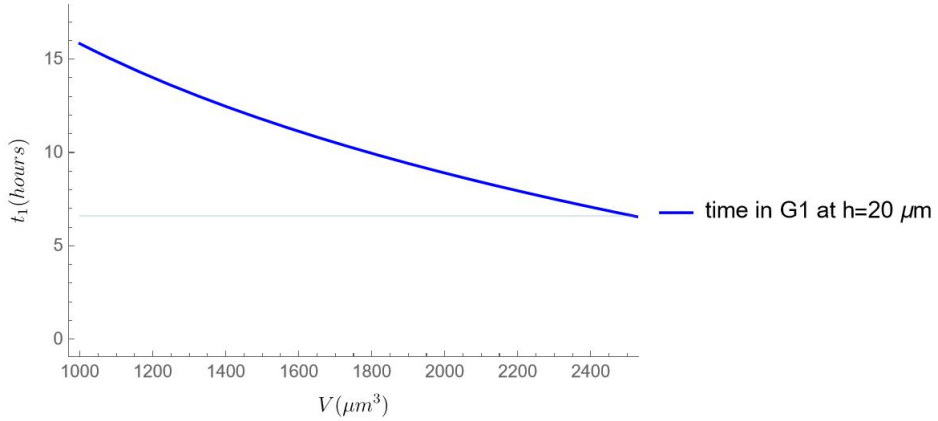

Figure 5.3: Time in G1 as a function of the total initial volume ($V_n + V_c$). At a confinement of h=20 μm the computation is done assuming a spherical shape.

It is worth mentioning that the theoretical model described in this work justifies the assumption of a sizer behaviour during cell growth.
This result can be deduced by looking at the plots in figure 5.4 and 5.5.
Figure 5.4 shows the final total volume ($V_c + V_n$) as a function of the volume at birth; as required for a sizer behaviour, the final volume does not depend on the volume at birth but is set at a specific value, in our case $V_f \sim 1200\mu m$.
Figure 5.5 instead shows the amount of volume added during the G1 phase for different values of the initial volume. There is clearly a negative correlation as predicted in figure 1.2(e). The slope of the curve is ~ -1, as expected from a sizer model.
The values used for the initial volume in these plots are in the range $1000 - 2200\mu m$.
In both cases the final volume has been obtained using formula 3.3 where all the parameters that depend on time are evaluated at the t_1 corresponding to a specific value of V_i.
Also the value of γ_c changes with the initial volume and can be obtained by solving equation 5.1 in γ_c keeping all the other terms fixed; indeed, since the critical tension γ_c represents the value of nuclear tension necessary to trigger the G1/S transition, when the condition $\gamma = \gamma_c$ is satisfied the cell can directly enter the S phase and $t_1 = 0$.
In our model this sizer behaviour comes from the prediction of a compensation mechanism that decreases the time in G1 as the volume at birth is larger, as seen in figure 5.3.

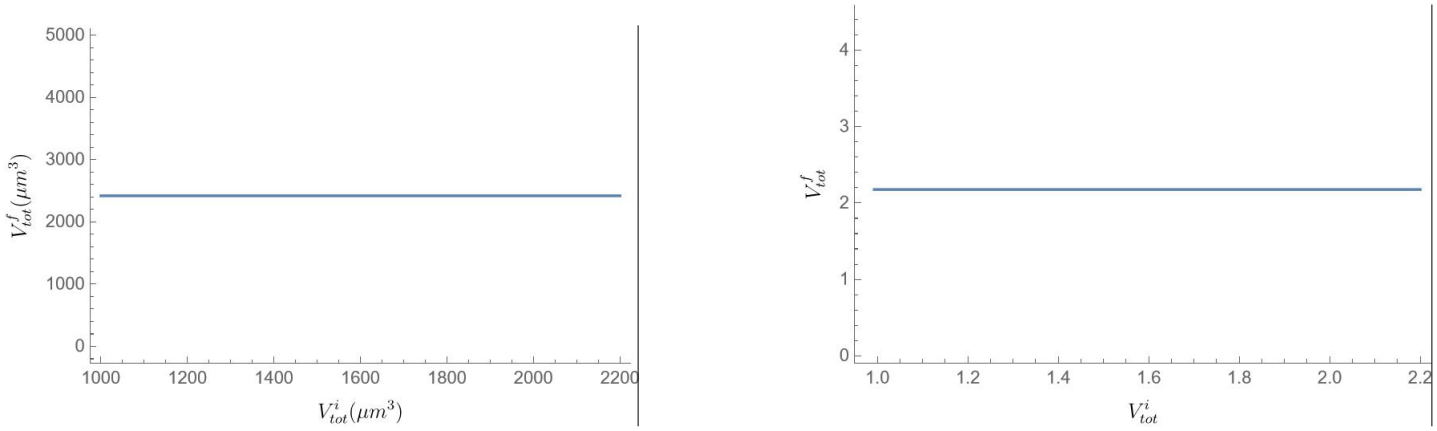

Figure 5.4: Final volume as a function of the initial volume.The plot on the right shows the values normalized by V_i.

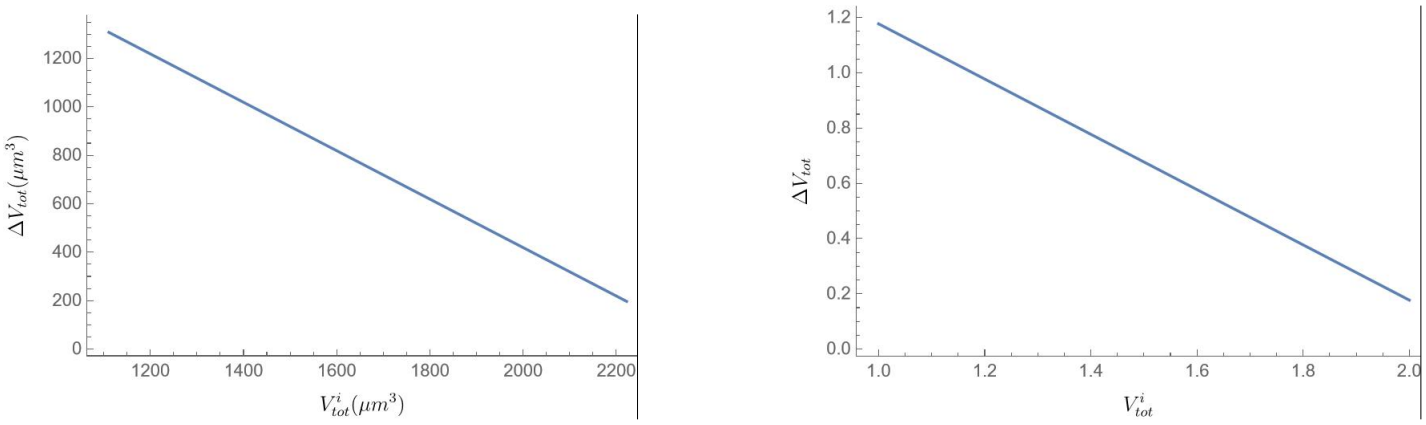

Figure 5.5: Added volume in the G1 phase with respect to the initial volume. In the plot on the right the volumes are normalized with respect to V_i.

Some interesting prediction that comes from our study and that can be verified experimentally can be identified.

For instance, in figure 5.2(b) we have pointed out the dependence of t_1 on the height of confinement h. This dependence can be combined with the one on the volume at birth as illustrated in figure 5.6.
What is observed is a shift of the curve that represents the dependence of t_1 on V_i as h is decreased. Intuitively this behaviour perfectly matches our prediction: stronger confinement, i.e. small h, implies a shape for the cell closer to a pancake than to a sphere with a consequent increasing surface; therefore, the critical value S^* related to the presence of a non-vanishing nuclear tension is reached before and

the G1/S transition is realized faster.

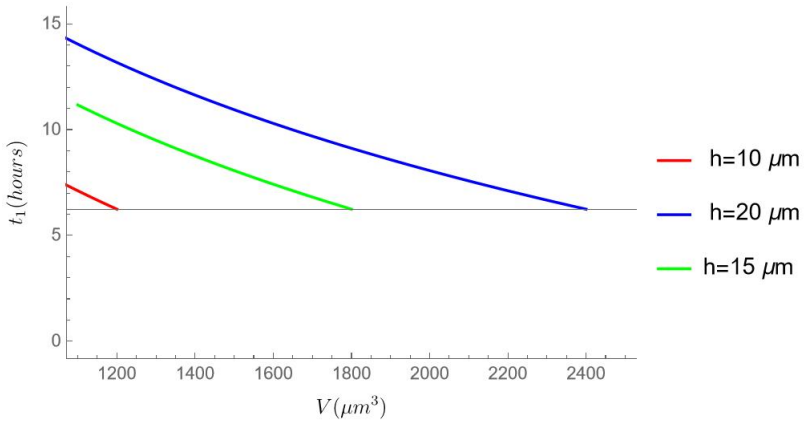

Figure 5.6: Time in G1 as the function of the initial volume V_i at different confinements h. The plot has a cut at a value $t_1 = 6$ hours since experimentally this is the minimum time that the cell has to spend in the G1 phase independently from its size and its confinement.

An interesting prediction is also the effect of a hyperosmotic/hyposmotic shock on t_1.
As described in the section dedicated to the Pump-Leak model, the osmotic pressure plays a crucial role in maintaining cell size homeostasis. As a consequence, a change in the concentration of the environment outside of the cell (i.e. a change in the parameter n_0) that affects the osmotic pressure will be relevant for the regulation of the cell cycle too.
In particular, two situations can be identified related to the variation of the osmotic pressure:

- hyperosmotic shock, when the external concentration n_0 increases and lead the cell to shrink;
- hyposmotic shock, when the concentration outside of the cell decreases with the effect of increasing the volume of the cell.

The results of these conditions on the length of the G1 phase are shown in figure 5.7.
As in the case of variable h analyzed previously, here again the curve that represents the time in G1 is shifted depending on the choice of the parameter n_0: larger n_0 (hyperosmotic shock) implies a decrease in the amount of time spent in the G1 phase at fixed initial volume since the outward osmotic pressure increases with a consequent increase in the nuclear tension; on the contrary, a smaller value of n_0

(hyposmotic shock) is related to an extension of the G1 phase due to an increase in the inward osmotic pressure and so a decrease in the nuclear tension.

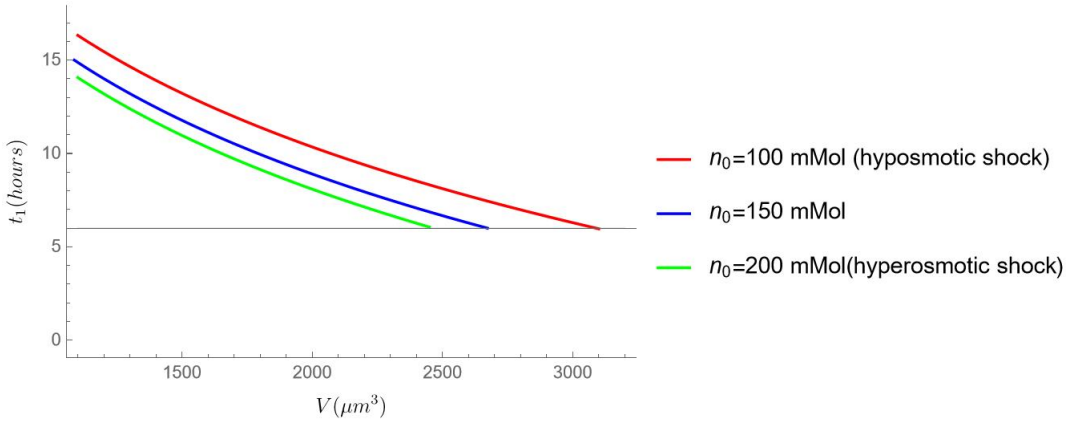

Figure 5.7: Effect of an osmotic shock on the time spent in the G1 phase.

Chapter 6

Conclusion

This report presents a first approach to the study of the relation between the scaling laws that govern cellular growth, the mechanisms that regulate them and their effect on the duration of the cell cycle.

Regarded as the main unit that constitutes life, the cell is a perfect example of how nature is capable of carrying out complex and delicate functions that to us, humans, seem hard to understand. Following the idea of starting from simple cases to get in the end an idea of a more complicated problem, the analysis of the regulation of the cell cycle represents the first step to understand how the growth of tissues and organisms in general is regulated and what triggers their dysfunction in the presence of anomalies and diseases.

Inspired by the evidence that the transition between different stages of the cell cycle is triggered by checkpoints, our study is focused on the first of this control mechanism, the one that separates the G1 from the S stage, that determines whether a cell is engaged into the cell cycle or it is stuck in a condition of quiescent. The key parameter that enables the cell to have a mechanism for proprioception and to respond to external forces appears to be the nucleus; known as the storage for the genetic material, the nucleus scales during growth coherently with the volume of the cell by keeping a specific NC ratio, which underlines its primary role in the transition between the stage of growth and the one of division. This transition seems to be related to the deformation of the nucleus, as in the case of cell migration, and it is strongly related to the balance of osmotic and hydrostatic pressure at the NE.
Indeed, the flattening of the nucleus beyond a critical value of the height of confinement determines an increase in the surface and a dramatic volume loss due to the presence of folds on the NE that act as a surface reservoir.

In this study, the attention is toward the tension that determines the starting of the S phase and seems to be the parameter that regulates the duration of cell growth. Based on this hypothesis, an analytical expression for the tension at the NE as a function of the height of the confinement has been derived both in the real case of small hydrostatic pressure and in the non-natural case of infinite hydrostatic pressure. The aim is to check the theoretical hypothesis of the relation between these two variables in defining the time spent in the G1 phase.
Once the tension has its analytical expression, the duration of G1 is derived by considering an exponential growth for the metabolites and the protein in the cell and in the nucleus, which is mathematically demonstrated by a stochastic model of gene expression coupled to a model for the maintenance of an osmotic equilibrium (PLM).
The result gives a value which is in agreement with experimental observations of a reduction of the cell cycle length in accordance with the volume of the cell at birth: bigger cells need less time to grow before dividing than smaller cells in the case of no confinement, while when flattening they all start division after the same amount of time spent in the G1 phase.

Even if successful as a first approximation, this study presents several limits: it considers only monovalent ions inside the cell and perfect pumping efficiency, i.e. all the anions are pumped outside of the cell; it does not take into account the middle stages in between the geometrical transition between a spherical shape of the nucleus before confinement and a pancake shape; it ignores the effect of the dry volume, a kind of excluded volume for the growth of the molecules in the cell and in the nucleus.

For example, if a larger pumping efficiency is considered (i.e. $\alpha_0 \neq 0$), a bigger amount of anions will be present inside the cell. As a consequence, the cell tends to swell and its volume increases.
A bigger volume may affect the critical value for the surface, S^*, at which the nuclear tension starts to be relevant by decreasing it with consequent shorter G1 phase.
This prediction of a logarithmic behaviour of the G1 length as a function of the critical surface could be an interesting result to compare with further experiments. It could provide more insights related to the behaviour of the NE and its folds.

An interesting question to answer would be to analyze how the results change when the dry volume, R, is added. Indeed, in this case even in the regime $\Delta P \to \infty$, when all the metabolites tend to leave the nucleus, there would still be this excluded volume that prevents the nuclear volume from vanishing. This difference would inevitably affect the tension that may not have a constant value.

Several improvements to this work may be considered.
As an example, the addition of noise could make the results more realistic; however it is not a simple task deciding which kind of noise, either multiplicative or additive, and to which parameter, either volume or number of protein etc.

Further improvements could bring attention to the understanding of the importance of the variety of nuclear shape and its fluctuations (the nucleus with no confinement presents a spherical shape only on average); to the study of the factors that determine the specific shape of the nucleus; to the nature of the NE itself and to the element of this membrane that responds to the tension during growth; to the link between the behaviour of the NE and its connection to the state of the chromatin inside the nucleus.
Answering these questions is a challenging problem and an opportunity to further proceed into the understanding of several diseases related to anomalies in cell growth.

Appendix A

Symbols

Parameter	Value
n_0	Concentration of metabolites outside of the cell (external osmolarity)
n^+	Cations concentration
n^-	Anions concentration
x	Metabolites concentration
z	Metabolites average charge
z_a	Amino-acids average charge
z_p	Proteins average charge
ΔP	Difference in hydrostatic pressure
π	Osmotic pressure inside the cell
π_0	Osmotic pressure outside the cell
$\Delta\pi$	Difference in osmotic pressure
kT	Thermal energy at T=300K. k stands for the Boltzmann constant $k = 1{,}380649 * 10^{-23} J/K^{-1}$
K	Stretching modulus of the lamina
V_n	Volume of the nucleus
V_c	Volume of the cell
R	Dry volume
S	Surface of the nucleus
S^*	Critical surface of the nucleus. Starting from this value the nuclear tension is non vanishing.
A_n/a_n	Number/concentration of amino-acids inside the nucleus
A_0	Total number of amino-acids inside the cell
A_c/a_c	Number/concentration of amino-acids in the cytoplasm

Parameter	Value
P_n/p_n	Number/concentration of protein inside the nucleus
P_c/p_c	Number/concentration of protein in the cytoplasm
P_{tot}	Total number of proteins
ϕ	Ratio of nuclear protein with respect to 0otal amount of protein inside the cell, i.e. $\frac{P_n}{P_n+P_c}$
Q/q	Number/concentration of chromatin counterions inside the nucleus
α_0	Pumping efficiency
α	Product $n_0 * S * h$
g^+	Conductivity of cations
p	Pumping of positive ions
X	Number of impermeant molecules inside the cell
M	Number of mRNA molecules
P	Number of proteins
r	Number of ribosomes
p_r	Number of RNAP molecules
τ_p	Degradation rate of proteins
τ_m	Degradation rate of mRNAs
ϕ_i	Ratio between gene i and the total amount of gene, i.e. $\frac{g_i}{\sum g_i}$
k_0	Rate of translation
k_t	Rate of transcription
k_{cat}	Rate of catalysis
e	Number of enzymes
l_p	Average protein length
k_r	Rate of growth for ribosomes, nuclear proteins and amino-acids in the exponential grow
γ	Nuclear tension
h	Height of confinement
R_0	Radius of the nucleus before confinement
β	Osmotic compressibility of the nucleus
κ	Bulk modulus of the nucleus

Table A.1: A table that summarizes all the symbols used in this thesis along with their meaning.

Appendix B

The Pump-Leak model

This section is aimed to give information about the background of the equations presented in the main text under the name of Pump-Leak model. Furthermore, the detailed solution to obtained equation 2.4 is discussed. A complete mathematical description of the problem can be found in [77] and [47].

B.1 Derivation and solution

While the origin of equation 2.1 and 2.2 is more clear from their meaning, the third equation 2.3 requires a small insight. Its root resides in the balance of the density of ionic current j_+/j_- :

$$\begin{cases} j_+ = -\Lambda_+ \nabla \mu_+ + p \\ j_- = -\Lambda_- \nabla \mu_- \end{cases} \tag{B.1}$$

Here we assume that only cations have an active contribution p. In these equations, known as the law of diffusion, $\Lambda_{+/-}$ are the conductances of cations and anions respectively while μ stands for the chemical potential. From thermodynamic considerations, the chemical potential can be seen as a sum of an entropic and a potential contribution, leading to

$$\begin{cases} j_+ = -\Lambda_+ (kT \log \frac{n_+}{n_0} + e\Psi) + p \\ j_- = -\Lambda_- (kT \log \frac{n_-}{n_0} - e\Psi) \end{cases} \tag{B.2}$$

with n_+, n_-, n_0 are ionic concentrations as seen in the main text and Ψ is the membrane potential. Because of the balance of ionic fluxes (i.e. $j_+ + j_- = 0$), if these two equations are divided by Λ_+ and Λ_- respectively and then summed up together, the result is

$$kT \log \frac{n_+ n_-}{n_0} + \frac{p}{\Lambda_+} = 0 \quad \rightarrow \quad \frac{n_+ n_-}{n_0} = \exp -\frac{p}{kT\Lambda_+} \quad \rightarrow \quad n_+ n_- = \alpha_0 n_0^2 \tag{B.3}$$

which is equivalent to equation 2.3.

From this equation and from equation 2.1 it is possible to obtain two different expressions for n_-:

$$\begin{cases} n_- = n_+ - z \cdot x \\ n_- = \alpha_0 \frac{n_0^2}{n_+} \end{cases} \tag{B.4}$$

By equating them, a quadratic equation for n_+ is derived

$$n_+^2 - z \cdot x n_+ - \alpha_0 n_0^2 = 0 \tag{B.5}$$

The solution is straightforward and allows to find an expression for the ionic concentration inside the cell as a function of the external ionic concentration and the concentration of impermeant molecules:

$$\begin{cases} n_+ = \frac{z \cdot x + \sqrt{(z \cdot x)^2 + 4\alpha_0 n_0^2}}{2} \\ n_+ = \frac{-z \cdot x + \sqrt{(z \cdot x)^2 + 4\alpha_0 n_0^2}}{2} \end{cases} \tag{B.6}$$

Once we have derived these expressions, we can simply substitute them in the equation for the balance of pressure 2.2 and we get the formula for the volume 2.4 in the case $\Delta P \sim 0$.
If instead the hydrostatic pressure is not negligible, as when it comes to the more interesting analyses of the nuclear volume, the formula takes the form:

$$\begin{cases} V = \frac{kTN_{tot}(\Delta P)}{(\pi_0 + \Delta P)} \\ \\ N_{tot}(\Delta P) = X \frac{z^2 - 1}{1 + \sqrt{1 + (z^2 - 1)\left(1 - \frac{\alpha_0}{(1 + \frac{\Delta P}{kT 2n_0})^2}\right)}} \end{cases} \tag{B.7}$$

Appendix C

Perturbation theory

In the main text, several results have been obtained thanks to the use of the perturbation theory. Here we give a general description of this method in order to make the procedure followed more clear. A complete description can be found in [78].

The main idea behind perturbation methods is to solve any problem by starting with its simplest version, which has a relatively simple solution, and adding to it a "perturbative part". The general solution x is usually given in terms of powers of a small parameter, ϵ, and it appears in the form:

$$x = x^0 + \epsilon x^1 + \epsilon^2 x^2 + ... \tag{C.1}$$

Since $\epsilon \to 0$, it is common costume to keep only the first order terms and to neglect the higher order terms, whose effect on the exact initial solution is gradually decreasing.

Following this convention, in the main text we have kept only the first order term in the equation for the amino-acids in the limit $\epsilon = \frac{\Delta P}{2n_0 kT} \to 0$ (see 3.12). Indeed, in these calculations the equation to solve to obtain an expression for the amino-acids as a function of the hydrostatic pressure is of the third order (see 3.11) so it is not directly solvable in an easy way. The solution can be computed instead by applying the perturbation method and it results in a zero-order term, which is the solution in the case $\Delta P = 0$, and higher order terms that depend on ΔP, which play the role of "corrections". In particular, since we decided to stop our calculation at the first order approximation, we have kept only power terms in $\frac{\Delta P}{2n_0 kT}$ and we have neglected terms in $\frac{\Delta P}{2n_0 kT}^2, \frac{\Delta P}{2n_0 kT}^3, ...$
In other words:

$$A_n^3 \to (A_n^0)^3 + 3(An_0)^2 A_n^1 \frac{\Delta P}{2n_0 kT} + 3A_n^0 (A_n^1)^2 \Big(\frac{\Delta P}{2n_0 kT}\Big)^2 + (A_n^1)^3 \Big(\frac{\Delta P}{2n_0 kT}\Big)^3 \tag{C.2}$$

becomes just

$$(A_n^0)^3 + 3(A_n^0)^2 A_n^1 \frac{\Delta P}{2n_0 kT} \tag{C.3}$$

and

$$A_n^2 \to (A_n^0)^2 + 2A_n^0 A_n^1 \frac{\Delta P}{2n_0 kT} + (A_n^1)^2 \Big(\frac{\Delta P}{2n_0 kT}\Big)^2 \tag{C.4}$$

becomes

$$(A_n^0)^2 + 2A_n^0 A_n^1 \frac{\Delta P}{2n_0 kT} \tag{C.5}$$

If we insert this new expression into equation 3.11 we get an equation where only the already known solution A_n^0 appears at the third order, while the unknown A_n^1 stops at the first order. The solution is obtained by solving first the zero-order term in ϵ, which gives equation 3.10, and then the first-order term, whose equation is in the form

$$-8(A_n^0)^3 + 8(P_c + P_n)A_n^0 A_n^1 + 8(A_0 + P_c - P_n - Q)(A_n^0)^2 - [4P_n A_0 - 4P_c(P_n + Q)] + (2P_n + Q)^2 A_n^1 - 8(P_c + A_0)(P_n + Q)A_n^0 = 0 \tag{C.6}$$

The solution is given in the main text (see equation 3.1.2).

C.1 Check of the results

As seen in the main text, the limit $Q = 0$, i.e. no chromatin counterions, is interesting to check the validity of the solution for A_n obtained through the perturbation method. If we follow the procedure described in the paragraph dedicated to the calculation of A_n, we have a volume

$$V_n = \frac{2A_n + 2P_n}{2n_0(1 + \frac{\Delta P}{2n_0 kT})} \tag{C.7}$$

With this formula for V_n the equation for A_n is of second order:

$$4\frac{\Delta P}{2n_0 kT} A_n^2 - \left[2(P_n + P_c) + 4\frac{\Delta P}{2n_0 kT}(A_0 + P_c)\right] A_n + 2A_0 P_n = 0 \tag{C.8}$$

with solution

$$A_n = \frac{2(P_n + P_c) + 4(\frac{\Delta P}{2n_0 kT})(A_0 + P_c) - \sqrt{\Big[2(P_n + P_c) + 4(\frac{\Delta P}{2n_0 kT})(A_0 + P_c)\Big]^2 - 32\frac{\Delta P}{2n_0 kT}A_0 P_n}}{8\frac{\Delta P}{2n_0 kT}} \tag{C.9}$$

which in the limit $\frac{\Delta P}{2n_0 kT} \to 0$ can be expanded in Taylor series and gives

$$\begin{aligned} A_n &= \frac{A_0 P_n}{(P_n + P_c) + 2\frac{\Delta P}{2n_0 kT}\Big[(A_0 + P_c) - A_0\frac{P_n}{P_n + P_c}\Big]} \\ &\to \quad A_0 \frac{P_n}{P_n + P_c}\Big\{1 + \Big(\frac{\Delta P}{2n_0 kT}\Big)\left[\frac{2A_0}{P_n}\Big(\frac{P_n}{P_n + P_c}\Big)^2 - \frac{2A_0}{P_n}\frac{P_n}{P_n + P_c}\right]\Big\} \end{aligned} \tag{C.10}$$

This result coincides with the one given by the perturbative approach (see equation 3.15).

Appendix D

Cell cycle

In physiology, the set of processes that leads one cell to become two is known as the *cell cycle*, following the principle *'Omnis cellula e cellula'* ("all cells (come) from cells")[79] formulated in 1858 by Rudolf Virchow, the father of the modern cellular pathology.

It was Murdoch Mitchison [1922–2011] who rewoke interest in the cell cycle with his book in 1971 "The Biology of the Cell Cycle" [80]. Nowadays, it is possible to identify two main levels of cell growth during the cell cycle:

1. the chromosome cycle during which DNA replicates and its content is separated into the two complete genomes of daughter nuclei;

2. the growth cycle which serves for the replication of all other components of a cell (e.g.proteins, membranes, organelles, etc.).

However, both stages share the need for an accurate mechanism of control. The chromosome cycle requires the genome to be carefully partitioned to daughter nuclei so that each new cell contains all the information necessary to keep the cell alive; a good regulation of the growth cycle is essential not to have cells progressively larger or smaller each generation with fatal consequences.

The eukaryotic cell cycle is divided into four main phases : the synthesis phase (S) (DNA replication and separation into two 'sister chromatids'), the mitosis phase (M) (prophase, metaphase, anaphase, telophase all participating in the effective cell division) and two growth phases (called "gap") in between (G1 and G2). Overall they constitute the generic cell cycle: G1–S–G2–M.

The alternation of the S and M phases is of fundamental importance. If a cell divide without finishing the phase of growth and DNA replication it will inherit incomplete genomes and either die or develop pathological behaviours [6].

A proper progression of the cell cycle is ensured by the existence of 'checkpoints', surveillance systems which prevent unwanted perturbations, such as DNA damage, nucleotide depletion or other defects. Of particular interest is the G1/S checkpoint (start or restriction point) since it is the point at which the cell 'decides' if to enter the cell cycle or not.
A newborn cell resides either in a quiescent state (G0), during which it does not divide, or in G1 until physiological parameters allow it to enter the S phase and start the replication of its genetic material. Loss of control over this regulatory system may result in several diseases (e.g. cancer [81], stroke [82]).

The importance of the G1 phase is underlined by its length; indeed, G1 is the stage with the most variable duration.
It has been found that for the characteristic cell cycle time of 20 hours in a HeLa cell, almost half is devoted to G1 and close to another half is S phase whereas G2 and M are much faster, at about 2-3 hours and 1 hour respectively [83].

The reason behind this variety of the G1 length has been identified in its relation to cell size regulation mechanisms [3] [84].
What remains to be investigated is the key factor that allows cells to couple their size homeostasis with the progression into the cell cycle, which is the main topic of this thesis.

Bibliography

[1] Teemu Miettinen, Matias Caldez, Philipp Kaldis, and Mikael Bjorklund. «Cell size control - a mechanism for maintaining fitness and function». In: *BioEssays* 39 (July 2017), p. 1700058. DOI: 10.1002/bies.201700058 (cit. on p. 1).

[2] Nicholas Rhind. «Cell-size control». In: *Current Biology* 31 (Nov. 2021), R1414–R1420. DOI: 10.1016/j.cub.2021.09.017 (cit. on pp. 1, 3, 4).

[3] Miriam Ginzberg, Ran Kafri, and Marc Kirschner. «Cell biology. On being the right (cell) size». In: *Science (New York, N.Y.)* 348 (May 2015), p. 1245075. DOI: 10.1126/science.1245075 (cit. on pp. 1, 61).

[4] Clotilde Cadart et al. «Size control in mammalian cells involves modulation of both growth rate and cell cycle duration». In: *Nature Communications* 9 (Aug. 2018). DOI: 10.1038/s41467-018-05393-0 (cit. on pp. 1, 2).

[5] Matthew Swaffer, Jacob Kim, Devon Chandler-Brown, Maurice Langhinrichs, Georgi Marinov, William Greenleaf, Anshul Kundaje, Kurt Schmoller, and Jan Skotheim. «Transcriptional and chromatin-based partitioning mechanisms uncouple protein scaling from cell size». In: *Molecular cell* 81 (Oct. 2021). DOI: 10.1016/j.molcel.2021.10.007 (cit. on pp. 1, 2, 16).

[6] John Devany, Martin Falk, Liam Holt, Arvind Murugan, and Margaret Gardel. «Tissue confinement regulates cell growth and size in epithelia». In: (July 2022). DOI: 10.1101/2022.07.04.498508 (cit. on pp. 1, 42, 60).

[7] Yuguang Xiong, Padmini Rangamani, Marc-Antoine Fardin, Azi Lipshtat, Benjamin Dubin-Thaler, Olivier Rossier, Michael Sheetz, and Ravi Iyengar. «Mechanisms Controlling Cell Size and Shape during Isotropic Cell Spreading». In: *Biophysical journal* 98 (May 2010), pp. 2136–46. DOI: 10.1016/j.bpj.2010.01.059 (cit. on p. 1).

[8] Xili Liu, Seungeun Oh, and Marc Kirschner. «The uniformity and stability of cellular mass density in mammalian cell culture». In: *Frontiers in Cell and Developmental Biology* 10 (Oct. 2022). DOI: 10.3389/fcell.2022.1017499 (cit. on p. 1).

[9] Shixuan Liu, Ceryl Tan, Chloe Melo-Gavin, Kevin Mark, Miriam Ginzberg, Ron Blutrich, Nish Patel, Michael Rape, and Ran Kafri. «Large cells activate global protein degradation to maintain cell size homeostasis». In: (2021). DOI: 10.1101/2021.11.09.467936. URL: https://doi.org/10.1101/2021.11.09.467936 (cit. on p. 1).

[10] Romain Rollin, Jean-François Joanny, and Pierre Sens. «Physical basis of the cell size scaling laws». In: *eLife* 12 (May 2023). DOI: 10.7554/eLife.82490 (cit. on pp. 1, 5, 15, 22, 24, 32).

[11] Paul Jorgensen and Mike Tyers. «How Cells Coordinate Growth and Division». In: *Current biology : CB* 14 (Jan. 2005), R1014–27. DOI: 10.1016/j.cub.2004.11.027 (cit. on p. 1).

[12] Gerald C. Johnston, John R. Pringle, and Leland H. Hartwell. «Coordination of growth with cell division in the yeast Saccharomyces cerevisiae.» In: *Experimental cell research* 105 1 (1977), pp. 79–98 (cit. on p. 2).

[13] PA Fantes and P Nurse. «Control of the timing of cell division in fission yeast. Cell size mutants reveal a second control pathway». In: *Experimental cell research* 115.2 (Sept. 1978), pp. 317–329. ISSN: 0014-4827. DOI: 10.1016/0014-4827(78)90286-0. URL: https://doi.org/10.1016/0014-4827(78)90286-0 (cit. on p. 2).

[14] *Cell Cycle | Introduction , Phases Checkpoints*. August 7,2019. URL: https://ibiologia.com/cell-cycle/ (cit. on p. 2).

[15] Masahito Tanaka and Shigehiko Yumura. «A 'Dynamic Adder Model' For Cell Size Homeostasis in Dictyostelium Cells». In: (Jan. 2021). DOI: 10.21203/rs.3.rs-152880/v1 (cit. on pp. 2, 4).

[16] Irina Pavelescu, Josep Vilarrasa-Blasi, Ainoa Planas Riverola, Mary Gonzalez Garcia, Ana Caño-Delgado, and Marta Ibañes. «A Sizer model for cell differentiation in Arabidopsis thaliana root growth». In: *Molecular Systems Biology* 14 (Jan. 2018), e7687. DOI: 10.15252/msb.20177687 (cit. on p. 2).

[17] Yuta Kitaguchi, Hajime Tei, and Koichiro Uriu. «Cell size homeostasis under the circadian regulation of cell division in cyanobacteria». In: *Journal of Theoretical Biology* 553 (Aug. 2022), p. 111260. DOI: 10.1016/j.jtbi.2022.111260 (cit. on p. 2).

[18] Sattar Taheri-Araghi, serena bradde serena, John Sauls, Norbert Hill, Petra Levin, johan paulsson johan, Massimo Vergassola, and Suckjoon Jun. «Cell-Size Control and Homeostasis in Bacteria [Curr Biol 2015] + data + extended Supplementary Information». In: *Current biology: CB* 25 (Dec. 2014). DOI: 10.1016/j.cub.2014.12.009 (cit. on p. 3).

[19] Frank Heldt, Reece Lunstone, John Tyson, and Bela Novak. «Dilution and titration of cell-cycle regulators may control cell size in budding yeast». In: (Apr. 2018). DOI: 10.1101/300160 (cit. on p. 3).

[20] Yanyan Chen, Rosa Baños, and Javier Buceta. «A Markovian Approach towards Bacterial Size Control and Homeostasis in Anomalous Growth Processes». In: *Scientific Reports* 8 (June 2018). DOI: 10.1038/s41598-018-27748-9 (cit. on p. 3).

[21] Jie Lin and Ariel Amir. «Homeostasis of protein and mRNA concentrations in growing cells». In: *Nature Communications* 9 (Oct. 2018). DOI: 10.1038/s41467-018-06714-z (cit. on pp. 4, 16, 17).

[22] Handuo Shi, Yan Hu, Pascal Odermatt, Carlos Gonzalez, Lichao Zhang, Joshua Elias, Fred Chang, and Kerwyn Huang. «Precise regulation of the relative rates of surface area and volume synthesis in bacterial cells growing in dynamic environments». In: *Nature Communications* 12 (Mar. 2021). DOI: 10.1038/s41467-021-22092-5 (cit. on p. 4).

[23] «Cyclin-dependent protein kinases: key regulators of the eukaryotic cell cycle.» In: *BioEssays* 17.6 (1995), pp. 471–480. DOI: 10.1002/BIES.950170603 (cit. on p. 4).

[24] Tobias Schmelzle and Michael N. Hall. «TOR, a Central Controller of Cell Growth». In: *Cell* 103 (2000), pp. 253–262 (cit. on p. 4).

[25] Alison Lloyd. «The Regulation of Cell Size». In: *Cell* 154 (Sept. 2013), pp. 1194–205. DOI: 10.1016/j.cell.2013.08.053 (cit. on p. 4).

[26] Evgeny Zatulovskiy, Shuyuan Zhang, Daniel Berenson, Benjamin Topacio, and Jan Skotheim. «Cell growth dilutes the cell cycle inhibitor Rb to trigger cell division». In: *Science (New York, N.Y.)* 369 (July 2020), pp. 466–471. DOI: 10.1126/science.aaz6213 (cit. on pp. 4, 7, 10).

[27] Balázs Enyedi, Mark Jelcic, and Philipp Niethammer. «The Cell Nucleus Serves as a Mechanotransducer of Tissue Damage-Induced Inflammation». In: *Cell* 165 (May 2016), pp. 1160–1170. DOI: 10.1016/j.cell.2016.04.016 (cit. on p. 4).

[28] Nicolas Andres Perez Gonzalez, Jiaxiang Tao, Nash Rochman, Dhruv Vig, Denis Wirtz, and Sean Sun. «Cell Tension and Mechanical Regulation of Cell Volume». In: *Molecular Biology of the Cell* 29 (Aug. 2018), mbc.E18–04. DOI: 10.1091/mbc.E18-04-0213 (cit. on p. 4).

[29] Ion Andreu et al. «Mechanical force application to the nucleus regulates nucleocytoplasmic transport». In: *Nature Cell Biology* 24 (June 2022), pp. 1–10. DOI: 10.1038/s41556-022-00927-7 (cit. on p. 5).

[30] Tyler J Kirby and Jan Lammerding. «Emerging views of the nucleus as a cellular mechanosensor». In: *Nature Cell Biology* 20 (Feb. 2018). DOI: 10.1038/s41556-018-0038-y (cit. on p. 5).

[31] Alexis Lomakin et al. «The nucleus acts as a ruler tailoring cell responses to spatial constraints». In: *Science (New York, N.Y.)* 370 (Oct. 2020). DOI: 10.1126/science.aba2894 (cit. on pp. 5, 7, 8, 21, 22).

[32] Valeria Venturini et al. «The nucleus measures shape changes for cellular proprioception to control dynamic cell behavior». In: *Science* 370 (6514 Oct. 2020). ISSN: 10959203. DOI: 10.1126/science.aba2644 (cit. on p. 5).

[33] Frank Neumann and Paul Nurse. «Nuclear size control in fission yeast». In: *The Journal of cell biology* 179 (Dec. 2007), pp. 593–600. DOI: 10.1083/jcb.200708054 (cit. on p. 5).

[34] Fabrizio Pennacchio et al. «Force-biased nuclear import sets nuclear-cytoplasmic volumetric coupling by osmosis». In: (June 2022). DOI: 10.1101/2022.06.07.494975 (cit. on p. 5).

[35] Julien Aureille et al. «Nuclear envelope deformation controls cell cycle progression in response to mechanical force». In: *EMBO Reports* (July 2019). DOI: 10.15252/embr.201948084 (cit. on pp. 7, 8, 21).

[36] Miriam Bracha Ginzberg, Nancy Chang, Heather D'Souza, Nish Patel, Ran Kafri, and Marc W Kirschner. «Cell size sensing in animal cells coordinates anabolic growth rates and cell cycle progression to maintain cell size uniformity». In: *eLife* 7 (June 2018). Ed. by Bruce Edgar, e26957. ISSN: 2050-084X. DOI: 10.7554/eLife.26957. URL: https://doi.org/10.7554/eLife.26957 (cit. on p. 10).

[37] DC Tosteson and JF Hoffman. «Regulation of cell volume by active cation transport in high and low potassium sheep red cells». In: *The Journal of general physiology* 44 (Sept. 1960), pp. 169–194. ISSN: 0022-1295. DOI: 10.1085/jgp.44.1.169. URL: https://europepmc.org/articles/PMC2195084 (cit. on p. 11).

[38] Ron Milo and Rob Phillips. *Cell Biology by the Numbers*. Dec. 2015. ISBN: 9781317230694. DOI: 10.1201/9780429258770 (cit. on pp. 11, 13, 15, 18, 25).

[39] Alan R. Kay and Mordecai P. Blaustein. «Evolution of our understanding of cell volume regulation by the pump-leak mechanism Journal of General Physiology [151, 4, April 1, (2019)] DOI: 10.1085/jgp.201812274». In: *Journal of General Physiology* 151 (4 Apr. 2019), pp. 606–607. ISSN: 15407748. DOI: 10.1085/jgp.201812274 (cit. on pp. 11, 12, 14).

[40] Gengqiang Xie, Reddick Walker, and Jerome Irianto. «Nuclear mechanosensing: mechanism and consequences of a nuclear rupture». In: *Mutation Research/Fundamental and Molecular Mechanisms of Mutagenesis* 821 (Aug. 2020), p. 111717. DOI: 10.1016/j.mrfmmm.2020.111717 (cit. on pp. 11, 21).

[41] Clay M. Armstrong. «The Na/K pump, Cl ion, and osmotic stabilization of cells». In: *Proceedings of the National Academy of Sciences* 100.10 (2003), pp. 6257–6262. DOI: 10.1073/pnas.0931278100. eprint: https://www.pnas.org/doi/pdf/10.1073/pnas.0931278100. URL: https://www.pnas.org/doi/abs/10.1073/pnas.0931278100 (cit. on pp. 11, 14).

[42] St. Szcz Zaleski. «Carl Schmidt». In: *Berichte der deutschen chemischen Gesellschaft* 27.4 (1894), pp. 963–978. DOI: https://doi.org/10.1002/cber.18940270494. eprint: https://chemistry-europe.onlinelibrary.wiley.com/doi/pdf/10.1002/cber.18940270494. URL: https://chemistry-europe.onlinelibrary.wiley.com/doi/abs/10.1002/cber.18940270494 (cit. on p. 11).

[43] Jens Chr. Skou. «The influence of some cations on an adenosine triphosphatase from peripheral nerves». In: *Biochimica et Biophysica Acta* 23 (1957), pp. 394–401. ISSN: 0006-3002. DOI: https://doi.org/10.1016/0006-3002(57)90343-8. URL: https://www.sciencedirect.com/science/article/pii/0006300257903438 (cit. on p. 11).

[44] Bryson Bennett, Elizabeth Kimball, Melissa Gao, Robin Osterhout, Steve Van Dien, and Joshua Rabinowitz. «Absolute Metabolite Concentrations and Implied Enzyme Active Site Occupancy in Escherichia coli». In: *Nature chemical biology* 5 (July 2009), pp. 593–9. DOI: 10.1038/nchembio.186 (cit. on p. 12).

[45] Håkan Wennerström, Eloy Vallina, Jens Danielsson, and Mikael Oliveberg. «Colloidal stability of the living cell». In: *Proceedings of the National Academy of Sciences* 117 (Apr. 2020), p. 201914599. DOI: 10.1073/pnas.1914599117 (cit. on p. 14).

[46] Frederick George Donnan. «Theory of membrane equilibria and membrane potentials in the presence of non-dialysing electrolytes. A contribution to physical-chemical physiology». In: *Journal of Membrane Science* 100 (1995), pp. 45–55 (cit. on p. 14).

[47] Zahra Aminzare and Alan Kay. «Mathematical modeling of ion homeostasis cell volume stabilization: impact of ion transporters, impermeant molecules, Donnan effect». In: (Dec. 2022). DOI: 10.1101/2022.12.08.519683 (cit. on pp. 14, 55).

[48] Larisa Venkova et al. «A mechano-osmotic feedback couples cell volume to the rate of cell deformation». In: *eLife* 11 (Apr. 2022). DOI: 10.7554/eLife.72381 (cit. on p. 15).

[49] Else Hoffmann and Ian Lambert. «Physiology of Cell Volume Regulation in Vertebrates». In: *Physiological reviews* 89 (Feb. 2009), pp. 193–277. DOI: 10.1152/physrev.00037.2007 (cit. on p. 15).

[50] Steven H. Strogatz. «Nonlinear Dynamics And Chaos». In: 1994 (cit. on p. 15).

[51] Harry A. Crissman and John Allan Steinkamp. «RAPID, SIMULTANEOUS MEASUREMENT OF DNA, PROTEIN, AND CELL VOLUME IN SINGLE CELLS FROM LARGE MAMMALIAN CELL POPULATIONS». In: *The Journal of Cell Biology* 59 (1973), pp. 766–771 (cit. on p. 16).

[52] Johan Paulsson. «Models of stochastic gene expression». In: *Physics of Life Reviews* 2 (2005), pp. 157–175 (cit. on p. 16).

[53] Micah Webster, Keren Witkin, and Orna Cohen-Fix. «Sizing up the nucleus: Nuclear shape, size and nuclear-envelope assembly». In: *Journal of cell science* 122 (June 2009), pp. 1477–86. DOI: 10.1242/jcs.037333 (cit. on pp. 20, 21).

[54] Christian Champy and H. M. Carleton. «Memoirs: Observations on the Shape of the Nucleus and its Determination». In: *Journal of Cell Science* 65 (1921), pp. 589–625 (cit. on pp. 20, 21).

[55] T Cavalier-smith. «Economy, speed and size matter: evolutionary forces driving nuclear genome miniaturization and expansion.» In: *Annals of botany* 95 1 (2005), pp. 147–75 (cit. on p. 20).

[56] R.T. Gregory. *The Evolution of the Genome*. Jan. 2005. DOI: 10.1016/B978-0-12-301463-4.X5000-1 (cit. on p. 20).

[57] Daniele Zink, Andrew Fischer, and Jeffrey Nickerson. «Nuclear structure in cancer cells». In: *Nature reviews. Cancer* 4 (Oct. 2004), pp. 677–87. DOI: 10.1038/nrc1430 (cit. on p. 20).

[58] Helena Santos-Rosa and Carlos Caldas. «Chromatin modifier enzymes, the histone code and cancer». In: *European journal of cancer (Oxford, England : 1990)* 41 (Dec. 2005), pp. 2381–402. DOI: 10.1016/j.ejca.2005.08.010 (cit. on p. 20).

[59] Howard J. Worman and J. C. Courvalin. «The nuclear lamina and inherited disease.» In: *Trends in cell biology* 12 12 (2002), pp. 591–8 (cit. on p. 20).

[60] B Futcher. «Cyclins and the wiring of the yeast cell cycle». In: *Yeast (Chichester, England)* 12.16 (Dec. 1996), pp. 1635–1646. ISSN: 0749-503X. DOI: 10.1002/(sici)1097-0061(199612)12:163c1635::aid-yea833e3.0.co;2-o (cit. on p. 20).

[61] Yufei Wu, Adrian Pegoraro, David Weitz, Paul Janmey, and Sean Sun. «The correlation between cell and nucleus size is explained by an eukaryotic cell growth model». In: *PLOS Computational Biology* 18 (Feb. 2022), e1009400. DOI: 10.1371/journal.pcbi.1009400 (cit. on p. 20).

[62] Monika Zwerger, Chin Yee Ho, and Jan Lammerding. «Nuclear Mechanics in Disease». In: *Annual review of biomedical engineering* 13 (Aug. 2011), pp. 397–428. DOI: 10.1146/annurev-bioeng-071910-124736 (cit. on pp. 21, 26).

[63] Dan Deviri and Samuel A. Safran. «Balance of osmotic pressures determines the nuclear-to-cytoplasmic volume ratio of the cell». In: *Proceedings of the National Academy of Sciences* 119.21 (2022), e2118301119. DOI: 10.1073/pnas.2118301119 (cit. on pp. 21, 22, 25).

[64] Joseph Long and Jan Lammerding. «Nuclear Deformation Lets Cells Gauge Their Physical Confinement». In: *Developmental Cell* 56 (Jan. 2021), pp. 156–158. DOI: 10.1016/j.devcel.2021.01.002 (cit. on pp. 21, 23).

[65] Michael Huber and Larry Gerace. «The size-wise nucleus: Nuclear volume control in eukaryotes». In: *The Journal of cell biology* 179 (Dec. 2007), pp. 583–4. DOI: 10.1083/jcb.200710156 (cit. on p. 22).

[66] Pierre Simon Laplace. *Traité de mécanique céleste, 1.* Typ. Crapelet, 1823 (cit. on pp. 21, 32).

[67] Michael Feig, Ryuhei Harada, Takaharu Mori, Isseki Yu, Koichi Takahashi, and Yuji Sugita. «Complete atomistic model of a bacterial cytoplasm for integrating physics, biochemistry, and systems biology.» In: *Journal of molecular graphics & modelling* 58 (2015), pp. 1–9 (cit. on p. 24).

[68] Sean McGuffee and Adrian Elcock. «Diffusion, Crowding Protein Stability in a Dynamic Molecular Model of the Bacterial Cytoplasm». In: *PLoS computational biology* 6 (Mar. 2010), e1000694. DOI: 10.1371/journal.pcbi.1000694 (cit. on p. 24).

[69] Robert D. Moir, Timothy P. Spann, Reynold I. Lopez-Soler, Miri Yoon, Anne E. Goldman, Satya Khuon, and Robert D. Goldman. «Review: The Dynamics of the Nuclear Lamins during the Cell Cycle— Relationship between Structure and Function». In: *Journal of Structural Biology* 129.2 (2000), pp. 324–334. ISSN: 1047-8477. DOI: https://doi.org/10.1006/jsbi.2000.4251. URL: https://www.sciencedirect.com/science/article/pii/S1047847700942515 (cit. on p. 26).

[70] Christophe Guilluy, Lukas D. Osborne, Laurianne Van Landeghem, Lisa Sharek, Richard Superfine, Rafael García-Mata, and Keith Burridge. «Isolated nuclei adapt to force and reveal a mechanotransduction pathway in the nucleus». In: *Nature Cell Biology* 16 (2014), pp. 376–381 (cit. on p. 26).

[71] Helena Cantwell and Gautam Dey. «Nuclear size and shape control». In: *Seminars in Cell Developmental Biology* 130 (Nov. 2021). DOI: 10.1016/j.semcdb.2021.10.013 (cit. on p. 33).

[72] Paula González Avalos, Michaela Reichenzeller, Roland Eils, and Evgeny Gladilin. «Probing compressibility of the nuclear interior in wild-type and lamin deficient cells using microscopic imaging and computational modeling». In: *Journal of Biomechanics* 44.15 (2011), pp. 2642–2648. ISSN: 0021-9290. DOI: https://doi.org/10.1016/j.jbiomech.2011.08.014. URL: https://www.sciencedirect.com/science/article/pii/S0021929011005628 (cit. on p. 40).

[73] E. GLADILIN, M. SCHULZ, C. KAPPEL, and R. EILS. «Contactless determination of nuclear compressibility using 3D image- and model-based analysis of drug-induced cellular deformation». In: *Journal of Microscopy* 240.3 (2010), pp. 216–226. DOI: https://doi.org/10.1111/j.1365-2818.2010.03394.x. eprint: https://onlinelibrary.wiley.com/doi/pdf/10.1111/j.1365-2818.2010.03394.x. URL: https://onlinelibrary.wiley.com/doi/abs/10.1111/j.1365-2818.2010.03394.x (cit. on p. 40).

[74] J. A. Smith and L. Martin. «Do Cells Cycle?» In: *Proceedings of the National Academy of Sciences* 70.4 (1973), pp. 1263–1267. DOI: 10.1073/pnas.70.4.1263 (cit. on p. 41).

[75] Giulia Varsano, Yuedi Wang, and Min Wu. «Probing Mammalian Cell Size Homeostasis by Channel-Assisted Cell Reshaping». In: *Cell Reports* 20 (July 2017), pp. 397–410. DOI: 10.1016/j.celrep.2017.06.057 (cit. on p. 41).

[76] Cesar Vargas-Garcia, Mikael Bjorklund, and Abhyudai Singh. «Modeling homeostasis mechanisms that set the target cell size». In: *Scientific Reports* 10 (Aug. 2020). DOI: 10.1038/s41598-020-70923-0 (cit. on p. 41).

[77] Yoichiro Mori. «Mathematical Properties of Pump-Leak Models of Cell Volume Control and Electrolyte Balance». In: *Journal of Mathematical Biology* 64 (Apr. 2011). DOI: 10.1007/s00285-011-0483-8 (cit. on p. 55).

[78] Mark H. Holmes. «Introduction to Perturbation Methods». In: 1995 (cit. on p. 57).

[79] Virchow Rudolf. *Cellular pathology: as based upon physiological and pathological histology twenty lectures delivered in the Pathological Institute of Berlin.* 1860 (cit. on p. 60).

[80] J. M. Mitchison. *The biology of the cell cycle.* 1971 (cit. on p. 60).

[81] Arthur Beck Pardee. «G1 events and regulation of cell proliferation.» In: *Science* 246 4930 (1989), pp. 603–8 (cit. on p. 61).

[82] Rui Lan Zhang, Zheng Gang Zhang, Mei Lu, Ying Wang, James J Yang, and Michael Chopp. «Reduction of the Cell Cycle Length by Decreasing G1 Phase and Cell Cycle Reentry Expand Neuronal Progenitor Cells in the Subventricular Zone of Adult Rat after Stroke». In: *Journal of Cerebral Blood Flow & Metabolism* 26.6 (2006). PMID: 16251885, pp. 857–863. DOI: 10.1038/sj.jcbfm.9600237. eprint: https://doi.org/10.1038/sj.jcbfm.9600237. URL: https://doi.org/10.1038/sj.jcbfm.9600237 (cit. on p. 61).

[83] Angela T. Hahn, Joshua T. Jones, and Tobias Meyer. «Quantitative analysis of cell cycle phase durations and PC12 differentiation using fluorescent biosensors». In: *Cell Cycle* 8 (2009), pp. 1044–1052 (cit. on p. 61).

[84] Seth M. Rubin, Julien Sage, and Jan M. Skotheim. «Integrating Old and New Paradigms of G1/S Control». In: *Molecular Cell* 80.2 (2020), pp. 183–192. ISSN: 1097-2765. DOI: https://doi.org/10.1016/j.molcel.2020.08.020. URL: https://www.sciencedirect.com/science/article/pii/S1097276520306055 (cit. on p. 61).